Influence of turbulent mixing on critical behavior of directed percolation process: Effect of compressibility

J. Honkonen,[1] T. Lučivjanský,[2,3] and V. Škultéty[4]
[1]*National Defence University, 00861 Helsinki, Finland*
[2]*Faculty of Sciences, P.J. Šafárik University, 04154 Košice, Slovakia*
[3]*Peoples' Friendship University of Russia (RUDN University), 6 Miklukho-Maklaya St, Moscow, 117198, Russian Federation*
[4]*Department of Physics, Stockholm University, AlbaNova University Center, SE-106 91 Stockholm, Sweden*

(Received 16 November 2017; published 15 February 2018)

Universal behavior is a typical emergent feature of critical systems. A paramount model of the nonequilibrium critical behavior is the directed bond percolation process that exhibits an active-to-absorbing state phase transition in the vicinity of a percolation threshold. Fluctuations of the ambient environment might affect or destroy the universality properties completely. In this work, we assume that the random environment can be described by means of compressible velocity fluctuations. Using field-theoretic models and renormalization group methods, we investigate large-scale and long-time behavior. Altogether, 11 universality classes are found, out of which 4 are stable in the infrared limit and thus macroscopically accessible. In contrast to the model without velocity fluctuations, a possible candidate for a realistic three-dimensional case, a regime with relevant short-range noise, is identified. Depending on the dimensionality of space and the structure of the turbulent flow, we calculate critical exponents of the directed percolation process. In the limit of the purely transversal random force, critical exponents comply with the incompressible results obtained by previous authors. We have found intriguing nonuniversal behavior related to the mutual effect of compressibility and advection.

DOI: 10.1103/PhysRevE.97.022123

I. INTRODUCTION

Nonequilibrium systems constitute a fascinating branch of physics, which encompasses many natural phenomena. In the last decades, a lot of effort has been put into study of different aspects, but still a general theory is lacking [1–3].

The directed bond percolation (DP) process also known as the Gribov process is a paradigmatic example, in which an absorbing phase transition between an active (fluctuating) and an inactive (absorbing) state occurs. At this transition, vigorous spatiotemporal fluctuations of the order parameter dominate. The resulting collective behavior is analogous to equilibrium phase transitions [4–7]. The main difference is in the scaling of the time variable different from that of the spatial variables [3,8]. The DP process describes creation of fractal percolation structures [9,10]. In high energy physics, the DP process was developed in a different context of Reggeon field theory with aim to describe behavior of hadrons. Later, it became clear that DP and Reggeon field theory are just different versions of the same critical theory. In complex nonequilibrium models, nonlinearities pose a crucial challenge for a theoretical description. In order to make a model mathematically amenable, one can either exploit a certain special feature or implement a sophisticated numerical scheme. The former approach is realized in the critical domain of DP, where correlated regions of microscopic degrees of freedom can be conveniently described by means of continuous fields.

As Janssen and Grassberger conjecture [11,12], necessary conditions for a system to be in DP universality class are (i) a single absorbing state, (ii) short-ranged interactions, (iii) a positive order parameter, and (iv) no additional symmetry or coupling with other slow variables. Several models have been identified and their adherence to the DP class has been shown, e.g., reaction-diffusion problems [13], percolation processes [14], hadron interactions [9].

Among the conditions of the DP universality class, point (iv) is very subtle from the experimental point of view. In realistic situations, impurities and defects, which are not taken into account in the original DP formulation, are expected to induce violations of universal properties of the model. This is believed to be one of the reasons why there are not so many direct experimental realizations [15–18] of the percolation process itself. A study of deviations from the ideal situation could proceed in different routes and this still constitutes a topic of an ongoing debate [8]. A substantial effort has been made in studying a long-range interaction using Lévy flights [19–21], effects of immunization [14,22], or in the presence of spatially quenched disorder [23]. In general, a behavior is observed with a possibility that the critical behavior is lost. For instance, the presence of quenched disorder in the latter case causes a shift of the critical fixed point to the unphysical region. This leads to such interesting phenomena as activated dynamical scaling or Griffiths singularities [24–27].

In this paper, we address the question as to how DP is affected by velocity fluctuations of an ambient environment in which DP takes place (qualitatively displayed in Fig. 1). Velocity fluctuations are hardly avoidable in any of laboratory experiments. For instance, a vast majority of chemical reactions occurs at finite temperature, which is inevitably accompanied by the presence of a thermal noise. Furthermore, disease spreading and chemical reactions may be affected heavily by turbulent advection [28,29]. In general, turbulence

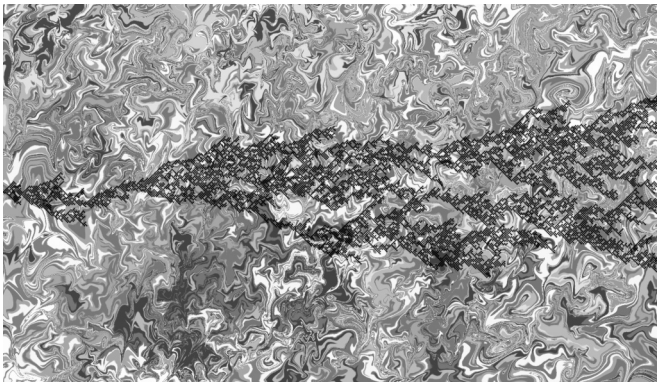

FIG. 1. Schematic visualization of the DP process in the presence of the fully developed turbulent flow. The black path represents the DP process (starting from the left and going rightwards) and the fully developed turbulence is displayed in the background.

is a rule rather than an exception and many physical phenomena cannot be properly explained without turbulence [30–33]. Here, our aim is to estimate how strong compressibility of the ambient fluid affects the DP process and what the main differences from the incompressible case [34–37] are.

For an analytic description of steady turbulent flow, it is customary to consider randomly forced (stochastic) Navier-Stokes equation [38–40]. In this framework, an important question is how properties of the random force affect the turbulent state. In case of incompressible turbulence, the random force is chosen to contain only transversal modes. Longitudinal modes generated by the nonlinearity of the Navier-Stokes equation are absorbed in fluctuations of pressure. In turbulence of compressible fluid, longitudinal modes of the velocity field are always present and have to be incorporated in a proper fashion. In our model, there is no influence of the percolating field on the velocity fluctuations. In other words, our model corresponds to the passive advection of the reacting scalar field.

Recently, there has been an increased interest in different advection problems in turbulent flows [41–44]. These studies have shown that compressibility plays a decisive role for population dynamics or chaotic mixing of colloids.

Our main aim in this paper is to elucidate to what extent strong compressible modes change the critical behavior of the DP universality class. To this end, we use a functional representation of the stochastic problem with the subsequent application of the field-theoretic renormalization group (RG) [4,5,7]. This theoretical framework allows us to examine asymptotic scaling behavior and infer quantitative predictions about universal quantities in a controllable fashion.

Let us note that there also exist different routes to tackle the problem. In particular, the nonperturbative (functional) renormalization group [5,45], numerical and simulation techniques, and approaches based on cellular automata [8,13] belong to important methods. The functional RG method has been successfully applied to the DP process [46,47], and separately to the incompressible Navier-Stokes equation [48,49]. Although feasible, the functional RG approach to compressible Navier-Stokes equation is still lacking. Intrinsic problems of reaction-diffusion models pose a challenge and are relevant for a proper construction of a coarse-grained theoretical model [50–52]. Here, we do not discuss such fundamental issues and start directly with a well-known phenomenological Langevin equation for the DP process [14].

This paper is organized as follows. In Sec. II A, we introduce a coarse-grained formulation of the DP problem, which we reformulate into the field-theoretic model. Also, we introduce relevant quantities we want to analyze. Next, in Sec. II B we provide a brief overview of the compressible Navier-Stokes equation and main differences to the incompressible case. Section III is reserved for the main steps of the renormalization group procedure. In Sec. IV, we present an analysis of possible regimes involved in the model. We analyze numerically and to some extent analytically fixed points' structure. In Sec. V, we give a concluding summary. Technical details concerning a calculation of the RG constants and functions are presented in Appendix A and Appendix B. Certain explicit expressions are summarized in Appendix C.

II. MODEL

A. Directed percolation

The field-theoretic formulation of the DP process may be obtained with the use of the Langevin equation [3,14]

$$\partial_t \psi = D_0(\partial^2 - R[\psi])\psi + \sqrt{\psi N[\psi]}f, \tag{1}$$

where $\psi = \psi(x)$ is the order parameter field (e.g., the density of species), $x = (\boldsymbol{x},t)$, D_0 is the microscopic (bare in the parlance of RG) diffusion constant, $\partial^2 = (\partial/\partial x_i)(\partial/\partial x_i) \equiv \partial_i\partial_i$ is the Laplace operator, $R[\psi]$ is a given time-local reaction functional which will be specified later, $N[\psi]$ is a local noise functional, and $f = f(x)$ is the random force with the following properties:

$$\langle f(x)\rangle = 0, \tag{2}$$

$$\langle f(x)f(x')\rangle = \delta(x - x'). \tag{3}$$

Note that Eq. (1) is a coarse-grained model that captures essential (universal) properties of DP only in the critical domain.

Further, it is important that the field $\psi(x)$ has been taken out from the functional $N[\psi]$ in Eq. (1) in order to obtain a multiplicative noise. This type of noise ensures that fluctuations vanish in the absorbing state $\psi = 0$, which is a fundamental property of models undergoing an active-to-absorbing phase transition [8,14]. In the critical domain, the density ψ is a slow variable and the reaction and the noise functional may be expanded as follows:

$$R[\psi] = \tau_0 + \lambda_0\psi/2 + \cdots, \tag{4}$$

$$N[\psi] = D_0\lambda_0 + \cdots, \tag{5}$$

where in the last expression we have extracted the diffusion constant D_0 due to dimensional reasons. The Langevin equation (1) then takes the form

$$\partial_t \psi = D_0(\partial^2 - \tau_0)\psi - D_0\lambda_0\psi^2/2 + \sqrt{D_0\lambda_0\psi}\, f\,. \tag{6}$$

In Eq. (6), the parameter τ_0 can be interpreted as the deviation from the percolation threshold (τ_0 is thus analogous to $\tau \propto (T - T_c)$, the deviation from the critical temperature in the φ^4

theory of static critical phenomena [4,5]), and λ_0 plays a role of a coupling constant. The subscript "0" denotes bare quantities for the future use of the RG method.

The field-theoretic formulation of the DP is given by the De Dominicis–Janssen response functional [53,54]

$$\mathcal{S}^{\psi}[\Phi_{\rm DP}] = \psi'\{\partial_t + D_0(\tau_0 - \partial^2)\}\psi + \frac{\lambda_0 D_0}{2}\{\psi - \psi'\}\psi'\psi, \tag{7}$$

where $\psi' = \psi'(x)$ is Martin-Siggia-Rose response field [55], $\Phi_{\rm DP} \equiv \{\psi', \psi\}$ is the set of all DP related fields in the response functional. The integration over all temporal and spatial variables is assumed, e.g., the first term on the right-hand side of Eq. (7) stands for

$$\psi'\partial_t\psi = \int dt \int d^d x\, \psi(\boldsymbol{x},t)\partial_t\psi(\boldsymbol{x},t). \tag{8}$$

The dynamic action (7) corresponds to the Itô interpretation of the stochastic differential equation (6) with the noise correlator (3). The field-theoretic formulation means that all correlations and response functions are represented as functional integrals with the functional measure $\mathcal{D}\psi\exp(-\mathcal{S}^{\psi}[\Phi_{\rm DP}])$. For instance, the pair connectedness function [8] is given by

$$\langle\psi'(x')\psi(x)\rangle = \int \mathcal{D}\psi'\mathcal{D}\psi\ \psi'(x')\psi(x)\exp(-\mathcal{S}^{\psi}[\Phi_{\rm DP}]). \tag{9}$$

Quantities of primary importance are the number of particles $N(t)$, radius of gyration $R^2(t)$, density of species $\rho(t)$, and the survival probability $P(t)$ defined as follows [8,14]:

$$\mathcal{N}(t) = \int d^d x\, \boldsymbol{x}^2\langle\psi'(\boldsymbol{0},0)\psi(\boldsymbol{x},t)\rangle, \tag{10}$$

$$\mathcal{R}^2(t) = \mathcal{N}^{-1}\int d^d x\, \langle\psi'(\boldsymbol{0},0)\psi(\boldsymbol{x},t)\rangle, \tag{11}$$

$$\rho(t) = \langle\psi(\boldsymbol{x},t)\rangle, \tag{12}$$

$$\mathcal{P}(t) = -\lim_{k\to\infty}\langle\psi'(\boldsymbol{x},-t)e^{-k\int d^d x\,\psi(\boldsymbol{x},0)}\rangle. \tag{13}$$

Their asymptotic long-time behavior is governed by the following universal power laws:

$$N(t) \sim t^{\Theta}, \quad \rho(t) \sim t^{-\delta}, \tag{14}$$

$$R^2(t) \sim t^{\tilde{z}}, \quad P(t) \sim t^{-\delta'}. \tag{15}$$

Numerical values of the corresponding critical exponents in the mean-field approximation read as

$$\Theta = 0, \quad \tilde{z} = 1, \quad \delta = \delta' = 1, \tag{16}$$

where the last equality follows from the rapidity symmetry [14], i.e., from the fact that the response functional (7) is invariant with respect to the transformation

$$\psi(\boldsymbol{x},t) \leftrightarrow -\psi'(\boldsymbol{x},-t). \tag{17}$$

B. Turbulent advection

In order to study the advection of DP by the random velocity field, let us recall that we have to replace the time derivative with the generalized covariant derivative [56,57]

$$\partial_t \to \nabla_t + a_0(\boldsymbol{\nabla}\cdot\boldsymbol{v}), \tag{18}$$

where $\nabla_t \equiv \partial_t + (\boldsymbol{v}\cdot\boldsymbol{\nabla})$ is the standard convective derivative and the parameter a_0 has to be introduced only in the case of compressible velocity field [58]. Permissible physical (microscopic and bare) values of this parameter are $a_0 = 0$ and 1, where the corresponding Langevin equation describes either an advection of the tracer field or an advection of the density field, respectively [56]. Effectively, this discussion leads to an additional term in the response functional (7) of the following form:

$$\mathcal{S}^{\rm adv}[\psi',\psi,\boldsymbol{v}] = \psi'(\boldsymbol{v}\cdot\boldsymbol{\nabla})\psi + a_0\psi'(\boldsymbol{\nabla}\cdot\boldsymbol{v})\psi. \tag{19}$$

Introduction of the velocity field in action (7) may generally break down the rapidity symmetry (17) which increases the number of independent critical exponents to four. However, as it has been shown previously in the case of compressible Kraichnan-velocity ensemble [58], this symmetry has to be modified

$$\psi(\boldsymbol{x},t) \leftrightarrow \psi'(-\boldsymbol{x},-t), \quad a_0 \to (1-a_0), \quad \lambda_0 \to -\lambda_0, \tag{20}$$

in order to ensure the number of independent exponents to remain three. The sign of the coupling constant λ also appears to be unimportant since the parameter of the perturbation expansion is λ^2 rather than λ.

In the present case, the velocity field is generated by the compressible NS (cNS) equation [59–61], written in the component form as

$$\rho\nabla_t v_i = \mu_0(\delta_{ij}\partial^2 - \partial_i\partial_j/3)v_j + \zeta_0\partial_i\partial_j v_j - \partial_i p_i + \rho f_i^{\boldsymbol{v}}, \tag{21}$$

augmented with the continuity equation

$$\partial_t\rho = -\partial_i(\rho v_i), \tag{22}$$

where $\rho = \rho(x)$ is the density field, $v = v(x)$ is velocity field and $p = p(x)$ is the pressure field of the fluid, μ_0 and ζ_0 are the dynamical and the bulk viscosity. Density of the random force per unit mass $f_i^{\boldsymbol{v}} = f_i^{\boldsymbol{v}}(x)$ mimics an energy input into the system [7,60], which is necessary to compensate a loss of energy due to viscous forces. In order to obtain a closed set of equations, we further assume the isothermal condition to hold. It relates the density and pressure of the fluid in the following way:

$$(p - \overline{p}) = c_0^2(\rho - \overline{\rho}). \tag{23}$$

Here, $\overline{p},\overline{\rho}$ denote the mean pressure and the mean density and c_0 is the speed of sound. Equations (21) and (22) can be then cast into a more convenient form

$$\nabla_t v_i = \nu_0(\delta_{ij}\partial^2 - \partial_i\partial_j)v_j + \nu_0 u_0\partial_i\partial_j v_j - \partial_i\phi + f_i^{\boldsymbol{v}}, \tag{24}$$

$$\nabla_t\phi = -c_0^2(\partial_i v_i), \tag{25}$$

where $\nu_0 = \eta_0/\overline{\rho}$ is the kinematic viscosity (see [60] for more details), u_0 is a new parameter related to the bulk viscosity via relation $\nu_0(u_0 - 1) = -\nu_0/3 + \zeta_0/\overline{\rho}$ and we have introduced a new density-related field $\phi = c_0^2\ln(\rho/\overline{\rho})$. In Eq. (24), the

specific random force $f_i^{\boldsymbol{v}}$ obeys Gaussian statistics with zero mean and the two-point correlator [61]

$$\left\langle f_i^{\boldsymbol{v}}(x) f_j^{\boldsymbol{v}}(x')\right\rangle = \frac{\delta(t-t')}{(2\pi)^d}\int_{k>m} d^d k\, D_{ij}^{\boldsymbol{v}}(\boldsymbol{k}) e^{i\boldsymbol{k}\cdot(\boldsymbol{x}-\boldsymbol{x}')}, \quad (26)$$

where m plays a rôle of the infrared (IR) cutoff and the spectrum $D_{ij}^{v}(\boldsymbol{k})$ is adopted in the form

$$D_{ij}^{\boldsymbol{v}}(\boldsymbol{k}) = g_{10} v_0^3 k^{4-d-y}[P_{ij}(\boldsymbol{k}) + \alpha Q_{ij}(\boldsymbol{k})] + g_{20} v_0^3. \quad (27)$$

Here, g_{10}, g_{20} are coupling constants, $P_{ij}(\boldsymbol{k}) = \delta_{ij} - k_i k_j/k^2$ and $Q_{ij}(\boldsymbol{k}) = k_i k_j/k^2$ are transversal and longitudinal projection operators, d is the dimension of the space, and y is an analytic regulator that serves as an expansion parameter in the perturbative RG [7,62]. The parameter y is analogous to the classical $\varepsilon = 4 - d$ in the theory of critical phenomena, which is introduced in order to regularize the ultraviolet (UV) divergences in the Feynman diagrams of the perturbative expansion. This procedure is also referred to as an analytic regularization [7]. The physically most relevant value of y is 4, where the trace of the nonlocal part of Eq. (26) becomes proportional to $\delta(\boldsymbol{k})$, which mimics the energy input from the largest spatial scales $\boldsymbol{k} \to 0$ [40].

The first term on the right-hand side in Eq. (27) represents a classical way of introducing the random force in the perturbative RG theory of turbulence, whereas the second term ensures the multiplicative renormalization of the model around $d = 4$ [61]. This point is discussed further in Sec. III B. The local part of the random-force correlation functions can be interpreted as a term responsible for thermal fluctuations (since in the real space it represents a delta correlated term that mimics the energy input from all spatial scales, including the smallest).

An important point to discuss here is the meaning of the parameter α, which is lacking in previous literature [60,61,63]. Let us consider the stochastic NS Eq. (21) in a slightly different form [56]

$$\partial_t(\rho v_i) + \partial_j(\rho v_i v_j) = \partial_j(\sigma'_{ij} - p\delta_{ij}) + \rho f_i^{\boldsymbol{v}}, \quad (28)$$

where σ'_{ij} is the viscous stress tensor responsible for the energy dissipation [56], whose exact form is unimportant at this stage. By taking the divergence of Eq. (28) with the subsequent insertion into the time derivative of the continuity equation (22) [together with the adiabatic condition (23)], we arrive at

$$\partial_{tt}^2\rho - c_0^2\partial^2\rho = \partial_i\partial_j(\rho v_j v_i - \sigma'_{ij}) - f_i^{\boldsymbol{v}}\partial_i\rho - \rho\partial_i f_i^{\boldsymbol{v}}. \quad (29)$$

This is nothing else (let alone the random force) than the Lighthill equation of aeroacoustics [57]. From Eq. (29), it is obvious that the longitudinal part of the random force is responsible for generation of sound waves. However, in the case of purely solenoidal random force ($\boldsymbol{\nabla}\cdot\boldsymbol{f}^{\boldsymbol{v}} = 0$) the sound waves may still be generated due to the nonlinearities on the right-hand side of Eq. (29). This implies that the sole limit $\alpha \to 0$ in Eq. (26) does not correspond to the incompressible limit. On the other hand, it has been shown within the one-loop approximation [60] that in the limit $\alpha \to 0$ the energy spectrum of the fully developed turbulence coincides with the Kolmogorov $-\frac{5}{3}$ law for the incompressible turbulence.

Using standard procedures [3,7,53] we finally obtain the De Dominicis–Janssen response functional

$$\begin{aligned}\mathcal{S}^{\boldsymbol{v}}[\Phi_{\rm vel}] = &-\frac{v_i' D_{ij}^{\boldsymbol{v}} v_j'}{2} + v_i'\{\nabla_t v_i - \nu_0[\delta_{ij}\partial^2 - \partial_i\partial_k]v_k \\ &- u_0\nu_0\partial_i\partial_j v_j + \partial_i\phi\} \\ &+ \phi'\left\{\nabla_t\phi - \tilde{v}_0\nu_0\partial^2\phi + c_0^2\partial_i v_i\right\}, \end{aligned} \quad (30)$$

where $\Phi_{\rm vel} \equiv \{\boldsymbol{v}', \boldsymbol{v}, \phi', \phi\}$ is a full set of velocity-related fields, $D_{ij}^{\boldsymbol{v}}$ is the velocity field random-force correlator (26), and we have added the term proportional to $\tilde{v}_0$ to establish the multiplicative renormalization [60].

The model for compressible turbulence based on compressible NS equation was for the first time proposed in [59]. However, as mentioned in [64,65] authors did not pay attention to the multiplicative renormalization and the model they obtained was not multiplicatively renormalizable as well as the term proportional to $\tilde{v}_0$ was omitted.

In contrast to the synthetic model for velocity field and its variations [29,66,67], the model (30) is Galilean invariant, which is specified in the next section. This leads to a restriction of possible terms that can be generated during the RG procedure and pose certain conditions on renormalization constants [37,68].

III. FIELD-THEORETIC RENORMALIZATION GROUP

A. Perturbation theory

The entire model describing the advection of the DP process in presence of compressible fully developed turbulence is given by the sum of response functionals (7), (19), and (30), briefly written as

$$\mathcal{S}[\Phi] = \mathcal{S}^{\psi} + \mathcal{S}^{\boldsymbol{v}} + \mathcal{S}^{\rm adv}, \quad (31)$$

where $\Phi = \Phi_{\rm DP} \cup \Phi_{\rm vel}$ is the set of all fields. Main objects of a practical interest are connected correlation functions $W_{\varphi\ldots\varphi}$ with $\varphi \equiv \varphi(x)$ being any permissible field from the set Φ. The generating functional $\mathcal{W}$ for connected correlation functions is customarily defined as [4,5,7]

$$\mathcal{W}[A] = \ln\mathcal{Z}[A], \quad G_{\varphi\ldots\varphi} = \left.\frac{\delta\mathcal{W}}{\delta\varphi\ldots\varphi}\right|_{A=0}, \quad (32)$$

where A stands for the set of source fields corresponding to Φ.

The building blocks of the perturbation theory are propagators and vertex factors. Propagators are acquired from the inverse of the quadratic part of the action functional (31):

$$\langle v_i v_j\rangle_0 = \frac{d_1^f}{|\epsilon_1|^2}P_{ij} + d_2^f\left|\frac{\epsilon_3}{R}\right|^2 Q_{ij}, \quad \langle\phi'\phi\rangle_0 = \frac{\epsilon_2^*}{R^*}, \quad (33)$$

$$\langle v_i' v_j\rangle_0 = \frac{1}{\epsilon_1^*}P_{ij} + \frac{\epsilon_3^*}{R^*}Q_{ij}, \quad \langle v_i'\phi\rangle_0 = \frac{ic_0^2 k_i}{R^*}, \quad (34)$$

$$\langle\phi\phi\rangle_0 = \frac{c_0^4 k^2}{|R|^2}d_2^f, \quad \langle v_i\phi'\rangle_0 = \frac{-ik_i}{R}, \quad (35)$$

$$\langle v_i\phi\rangle_0 = \frac{ic_0^2\epsilon_3 k_i}{|R|^2}d_2^f, \quad \langle\psi\psi'\rangle_0 = \frac{1}{L}, \quad (36)$$

where we have introduced the shorthand notation

$$\epsilon_1 = -i\omega + \nu_0 k^2, \quad d_1^f = \nu_0^3(\alpha g_{10}k^{d-4-y} + g_{20}), \quad (37)$$

$$\epsilon_2 = -i\omega + \nu_0 u_0 k^2, \quad d_2^f = \nu_0^3(\alpha g_{10}k^{d-4-y} + g_{20}), \quad (38)$$

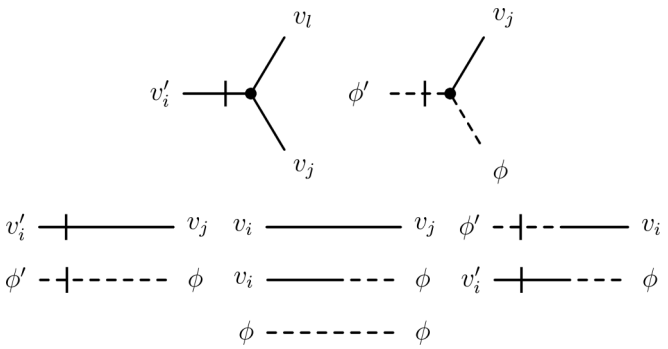

FIG. 2. Perturbation elements of the velocity part of model (31).

$$\epsilon_3 = -i\omega + \nu_0\tilde{\nu}_0 k^2, \quad L = -i\omega + \nu_0 w_0(k^2 + \tau_0), \tag{39}$$

$$R = \epsilon_1\epsilon_2 + c_0^2 k^4. \tag{40}$$

For brevity, we do not display the complex conjugate counterparts $\langle\varphi\varphi'\rangle = \langle\varphi'\varphi\rangle^*, \varphi \in \Phi$. All remaining free (unperturbed) correlation functions are identically zero. The vertex factors $V_{\varphi\ldots\varphi}$ are extracted from the interaction part of the response functionals (7) and (30):

$$V_{v_i' v_j(\boldsymbol{q}) v_l(\boldsymbol{k})} = -i(k_j\delta_{il} + q_l\delta_{ij}), \tag{41}$$

$$V_{\phi' v_j \phi(\boldsymbol{k})} = -ik_j, \tag{42}$$

$$V_{\psi'\psi'\psi} = -V_{\psi'\psi\psi} = \lambda_0 D_0, \tag{43}$$

$$V_{\psi' v_i(\boldsymbol{q})\psi(\boldsymbol{k})} = -i(k_i + a_0 q_i). \tag{44}$$

A graphical representation of the Feynman rules is depicted in Figs. 2 and 3. Apparently, theory (31) is translation invariant. For such theories it is convenient to work with the effective potential Γ, defined as the Legendre transform of $\mathcal{W}$ [5,69]:

$$\mathcal{W}[A] = \Gamma[\alpha] + A\alpha, \quad \alpha = \left.\frac{\delta\mathcal{W}[A]}{\delta A(x)}\right|_{A(x)=0}. \tag{45}$$

The effective action Γ also represents a generating functional for vertex functions $\Gamma_{\alpha\ldots\alpha}$. It can be shown [4,5,7] that after the relabeling $\alpha \to \Phi$ the relation between the effective potential and the original response functional takes the simple form

$$\Gamma[\Phi] = -\mathcal{S}[\Phi] + (\text{1I loop corrections}). \tag{46}$$

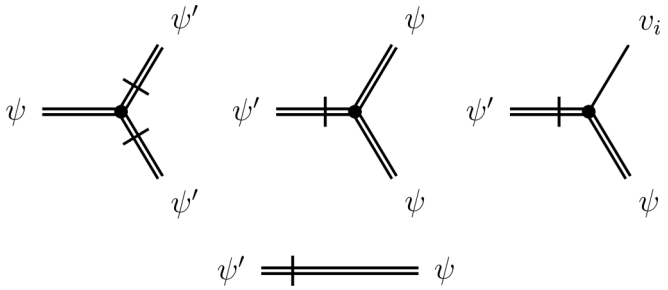

FIG. 3. Perturbation elements related to DP process and advecting interaction of model (31).

1I (one-irreducible) loop corrections in (46) are Feynman diagrams, which remain connected if one of the lines is removed. At the tree level we have $\Gamma_0[\Phi] = -\mathcal{S}_0[\Phi]$. The next-to-leading order requires a calculation of all one-loop Feynman diagrams. Such calculations are usually plagued with divergences, which can be taken care of with a proper renormalization scheme [5,7].

B. UV divergences and renormalization procedure

Renormalization of model (30) has been carried out both directly at $d = 3$ in [60] and with the use of a double expansion scheme in the vicinity of the space dimension $d = 4$ in [61]. Since the upper critical dimension of the DP model is four (the coupling constant of the DP becomes dimensionless, see below) we have to renormalize the cNS model around $d = 4$ as well. In field-theoretic models of passive turbulent advection or advection of models such as (7) the velocity field is not renormalized at all, which simplifies the RG procedure [34,40,58,63]. The same situation occurs also in the present case. Because the velocity model has been discussed in detail elsewhere [61] and it is not our main aim here, we do not dwell on the full renormalization procedure of the cNS model but discuss only topics relevant to our model.

The initial part of the RG procedure consists of an analysis of the UV divergences based on a calculation of canonical dimensions [4,5,7]. Dynamical models such as (7) and (30) have two independent length scales: spatial and temporal length scale. We introduce d_Q^k and d_Q^ω as the momentum and a frequency canonical dimension, respectively. Their linear combination

$$d_Q = d_Q^k + 2d_Q^\omega \tag{47}$$

denotes the total canonical dimension d_Q of the quantity Q. The total canonical dimension (47) plays the same role as a standard canonical dimension in static theories [4,5]. A list of all canonical dimensions for the current model is shown in Table I.

Superficial divergences are present in such 1I functions Γ, for which the UV exponent

$$\delta_\Gamma = d_\Gamma|_{\varepsilon=y=0} = 6 - \sum_\varphi N_\varphi d_\varphi \tag{48}$$

is non-negative. The sum in Eq. (48) runs over all field arguments of the function Γ.

To sort out 1I functions Γ with real UV divergences, the following properties of the model are utilized:

(a) 1I functions without at least one response field v', ϕ', and ψ' necessarily contain a closed loop of retarded propagators, and therefore no such counterterm can appear. Moreover, structures with at least one field ψ' must contain at least one field ψ. Otherwise, we obtain again a closed loop. A detailed technical exposition can be found in [7].

(b) Fields v and ϕ appear in interaction vertices of the action (30) together with their derivatives, and the real UV exponent is reduced according to

$$\delta_\Gamma' = \delta_\Gamma - n_v - n_\phi. \tag{49}$$

TABLE I. Canonical dimensions of all the bare fields and bare parameters for the model of velocity fluctuations. Parameters m and Λ are the IR and UV cutoff, respectively, and μ is the scale-setting parameter.

Q	$\boldsymbol{v}_0'$	$\boldsymbol{v}_0$	ϕ_0'	ϕ_0	ψ'	ψ	m,μ,Λ	τ	ν_0,ν,D_0,D	c_0,c	g_{10}	$g_{20},g_{30}=\lambda_0^2$	$u_0,v_0,w_0,u,v,w,g_1,g_2,g_3,\alpha_0,\alpha$
d_Q^k	$d+1$	-1	$d+2$	-2	$d/2$	$d/2$	1	2	-2	-1	y	ε	0
d_Q^ω	-1	1	-2	2	0	0	0	0	1	1	0	0	0
d_Q	$d-1$	1	$d-2$	2	$d/2$	$d/2$	1	2	0	1	y	ε	0

For instance, 1I function $\Gamma^{\psi'\psi\phi}$ has $\delta_\Gamma = 0$, but $\delta_\Gamma' = -1$, and therefore it is a finite function (does not require renormalization).

(c) The Galilean invariance [40,61] of model (30) ensures that the convective derivative ∇_t must enter the counterterms as a single object [7,60]. This implies that structures $\psi'\partial_t\psi$ and $\psi'(\boldsymbol{v}\cdot\boldsymbol{\nabla})\psi$ have to be renormalized by the same counterterm. An additional observation, which reduces possible types of counterterms, is the generalized Galilean invariance under the time-dependent transformation (instantaneous) velocity parameter $\boldsymbol{V}_i(t)$:

$$\begin{aligned} &\boldsymbol{v}_w(x) = \boldsymbol{v}(x_w) - \boldsymbol{V}_i(t), \quad x = (t,\boldsymbol{x}),\\ &\Phi_w(x) = \Phi(x_w); \quad x_w = (t,\boldsymbol{x}+\boldsymbol{V}(t));\\ &\boldsymbol{V}(t) = \int_{-\infty}^{t} \boldsymbol{V}_i(t')dt', \end{aligned} \tag{50}$$

where Φ stands for any of the three remaining fields: v',ϕ',ϕ. Despite the fact that the response functional is *not* invariant with respect to such a transformation, it transforms in the identical way with the generating functional of the one-irreducible Green functions

$$\begin{aligned} \mathcal{S}[\Phi_w] &= \mathcal{S}[\Phi] + \boldsymbol{v}'\cdot\partial_t\boldsymbol{V}_i,\\ \Gamma[\Phi_w] &= \Gamma[\Phi] + \boldsymbol{v}'\cdot\partial_t\boldsymbol{V}_i. \end{aligned} \tag{51}$$

The latter expression could be expressed in the form (46). In fact, the expression (51) means that the counterterms appear invariant under the generalized Galilean transformation (50).

(d) From the explicit form of the propagators in Eqs. (33) and (34), we observe that $\langle v'\phi\rangle_0$ and $\langle v\phi\rangle_0$ are proportional to c_0^2 while $\langle\phi\phi\rangle_0$ is proportional to c_0^4. On the other hand, propagator $\langle\phi\phi'\rangle_0$ is not proportional to any power of c_0. Since these factors have a positive total canonical dimension (see Table I), they appear as an external factor in a given Feynman diagram. Hence, the real UV exponent is reduced by the number of fields containing this factor. The vertex function with $N_{\phi'} > N_\phi$ contains factor $c_0^{2(N_{\phi'}-N_\phi)}$. For example, the Green function $\Gamma^{\psi'\psi\phi'}$ is UV finite because the UV exponent is reduced from $\delta_\Gamma = 0$ to $\delta_\Gamma' = -2$ [63].

As a consequence, we arrive at the conclusion that we can remove all UV divergences of the DP model by addition of the following counterterms:

$$\psi'\partial_t\psi, \quad \psi'\partial^2\psi, \quad \tau\psi'\psi, \quad \psi'(\boldsymbol{v}\cdot\boldsymbol{\nabla})\psi, \tag{52}$$

$$\psi'(\boldsymbol{\nabla}\cdot\boldsymbol{v})\psi, \quad \psi'\psi^2, \quad \psi'^2\psi\ . \tag{53}$$

All of these terms are already present in model (31), and thus the model is multiplicatively renormalizable.

In explicit terms, the renormalization of the DP response functional is accomplished by the following renormalization of the parameters and fields:

$$g_{30} = g_3\mu^\varepsilon Z_{g_3}, \quad D_0 = DZ_D, \quad \tau_0 = \tau Z_\tau + \tau_c, \tag{54}$$

$$\lambda_0 = \lambda\mu^{\varepsilon/2}Z_\lambda, \quad w_0 = wZ_w, \quad a_0 = aZ_a, \tag{55}$$

with the substitution $\psi' \to \psi' Z_{\psi'}$, $\psi \to \psi Z_\psi$ and similarly for the cNS field [60,61]. Note that the term τ_c is a nonperturbative effect [14,70,71], which is not captured by the dimensional regularization.

For completeness (details in [61]), we note that the following renormalization of the velocity part of the action (31) is needed:

$$\begin{aligned} &g_{10} = g_1\mu^y Z_{g_1}, \quad u_0 = uZ_u, \quad \nu_0 = \nu Z_\nu,\\ &g_{20} = g_2\mu^\varepsilon Z_{g_2}, \quad v_0 = vZ_v, \quad c_0 = cZ_c, \end{aligned} \tag{56}$$

supplemented with the renormalization of ϕ and ϕ' fields

$$\phi \to Z_\phi\phi, \quad \phi' \to Z_{\phi'}\phi'. \tag{57}$$

The total renormalized response functional of DP advected by compressible turbulent flow is then $\mathcal{S}_R = \mathcal{S}_R^\psi + \mathcal{S}_R^v + S_R^{\rm adv}$ explicitly given by

$$\begin{aligned} \mathcal{S}_R^\psi[\Phi] = {}& \psi'\{Z_1\partial_t + D(-Z_2\partial^2 + Z_3\tau)\}\psi\\ &- \frac{\lambda D}{2}\{Z_4\psi' - Z_5\psi\}\psi'\psi + \psi'\{Z_1 v_i\partial_i\\ &+ Z_6 a(\partial_i v_i)\}\psi, \end{aligned} \tag{58}$$

which has to be augmented by the relations for the renormalization constants

$$Z_1 = Z_{\psi'}Z_\psi, \quad Z_2 = Z_{\psi'}Z_\psi Z_D, \tag{59}$$

$$Z_3 = Z_{\psi'}Z_\psi Z_D Z_\tau, \quad Z_4 = Z_{\psi'}^2 Z_\psi Z_D Z_\lambda, \tag{60}$$

$$Z_5 = Z_{\psi'}Z_\psi^2 Z_D Z_\lambda, \quad Z_6 = Z_{\psi'}Z_\psi Z_a. \tag{61}$$

These relations can be easily inverted to express the RG constants of fields and parameters in terms of Z_i, $i = 1,\ldots,6$. In the one-loop approximation, the following diagrams are

required for the DP part of the total model (31):

$$\Gamma_{\psi'\psi} = i\omega Z_1 - Dk^2 Z_2 - D\tau Z_3 + \frac{1}{2}$$ 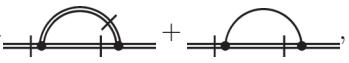 (62)

$$\Gamma_{\psi\psi'\psi'} = D\lambda\mu^{\frac{\varepsilon}{2}} Z_4 +$$ 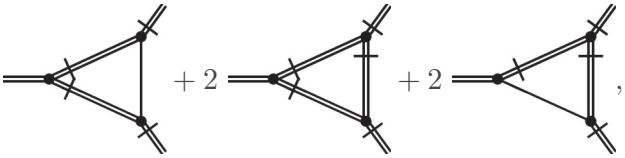 (63)

$$\Gamma_{\psi'\psi\psi} = -D\lambda\mu^{\frac{\varepsilon}{2}} Z_5 +$$ 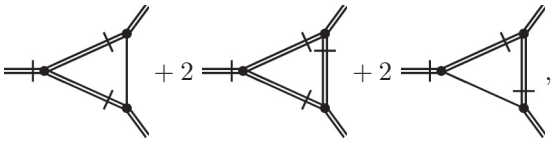 (64)

$$\Gamma_{\psi'\psi v_i} = -ip_i Z_1 - iq_i Z_6 +$$ 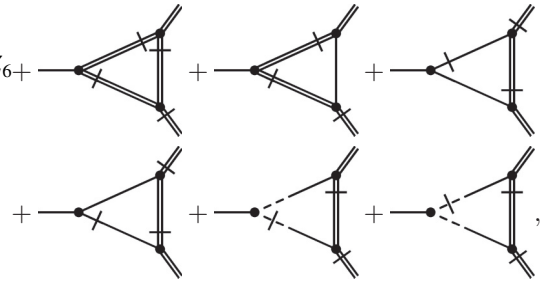 (65)

where p_i and q_i in the last equation stand for momenta of fields ψ and v_i, respectively. Passivity of the problem directly leads to the absence of additional corrections to cNS model caused by the DP perturbation elements. The explicit expressions for renormalization constants are given in Appendix A.

Investigation of the large-scale and long-time universal properties of the field-theoretic models calls for an analysis of Green functions at different spatiotemporal scales. The relation between the renormalized G and bare G_0 Green functions is the following [4,7]:

$$G_0^{\varphi'\varphi}(\{k_i\},e_0) = Z_{\varphi'}^{N_{\varphi'}}(g) Z_{\varphi}^{N_{\varphi}}(g) G^{\varphi'\varphi}(\{k_i\},e,\mu), \tag{66}$$

where φ,φ' stand for any permissible (physical or auxiliary) field, $k = (\boldsymbol{k},\omega)$ is a Euclidean four-vector, $g = g(\mu)$ is the full set of renormalized charges, and $e_0,e = e(\mu)$ are sets of all bare and renormalized parameters (including masses) with μ being the reference mass scale. In what follows, we denote the logarithmic derivative with respect to any quantity x as $\mathcal{D}_x \equiv x\partial_x$. Let us denote $\tilde{\mathcal{D}}_\mu$ the logarithmic derivative with respect to μ with fixed bare parameters. An application of $\tilde{\mathcal{D}}_\mu$ on both sides of Eq. (66) yields the fundamental RG equation [4,5]

$$\{\mathcal{D}_{\mathrm{RG}} + N_{\varphi'}\gamma_{\varphi'} + N_{\varphi}\gamma_{\varphi}\} G(\{k_i\},e,\mu) = 0, \tag{67}$$

where γ_Q is the anomalous dimension of the quantity Q:

$$\gamma_Q = \tilde{\mathcal{D}}_\mu \ln Z_Q. \tag{68}$$

Further, operator $\mathcal{D}_{\mathrm{RG}}$ in Eq. (67) is the $\tilde{\mathcal{D}}_\mu$ operator expressed in terms of renormalized parameters

$$\mathcal{D}_{\mathrm{RG}} = \mathcal{D}_\mu + \beta_g\partial_g - \gamma_v\mathcal{D}_v - \gamma_c\mathcal{D}_c - \gamma_\tau\mathcal{D}_\tau, \tag{69}$$

where in the second term summation over all charges g of theory is implied. For convenience, we denote by g the following set:

$$g = \{g_1,g_2,u,v,g_3,w,a\}. \tag{70}$$

The beta functions β_g, describing the dependence of charges on the reference mass scale μ, are defined as

$$\beta_g = \mathcal{D}_\mu g. \tag{71}$$

For the DP process advected by turbulent flow they are found from (54) and (55):

$$\beta_{g_3} = -g_3(\varepsilon + \gamma_{g_3}), \quad \beta_w = -w\gamma_w, \quad \beta_a = -a\gamma_a, \tag{72}$$

and similarly for charges of the cNS field [61]

$$\begin{aligned} \beta_{g_1} &= -g_1(y + \gamma_{g_1}), \quad \beta_{g_2} = -g_2(\varepsilon + \gamma_{g_2}), \\ \beta_u &= -u\gamma_u, \quad \beta_v = -v\gamma_v, \end{aligned} \tag{73}$$

which we quote here for completeness.

The explicit form of the RG functions can be found in Appendix B. The asymptotic behavior is described by the IR fixed point (FP) g^* at which all the charges satisfy

$$\forall\, g: \quad \beta_g(g^*) = 0. \tag{74}$$

Recall the abbreviations (70), so in fact Eq. (74) is a system of seven interconnected equations for seven unknowns. Stability of the given fixed point is then determined by eigenvalues of the matrix of the first derivatives

$$\Omega_{ij} = \left.\frac{\partial\beta_{g_i}}{\partial g_j}\right|_{g=g^*}. \tag{75}$$

In the case of IR attractive stable point, real parts of the eigenvalues of this matrix have to be strictly positive [7].

TABLE II. List of all fixed points. We use the following abbreviations ($\Delta = \{y,\varepsilon,\alpha\}$), $G(\Delta) = \frac{16y(2y-3\varepsilon)}{9((\alpha+2)y-3\varepsilon)}$, $H(\Delta) = \frac{16\alpha y^2}{9((\alpha+2)y-3\varepsilon)}$, $C = (\sqrt{13}-1)/2$ and NF stands for "not fixed," i.e., a coordinate is not determined in unambiguous fashion. Expressions that are not displayed are rather lengthy and a few explicit formulas can be found in Appendix C. Coordinates of the fixed-point values of cNS charges are taken from [61]. Further comments are found in the main text. Numerical values are rounded to five decimal places, where the last number in brackets denotes the last rounded digit.

FP/$g^*\|\lambda_i$	g_1^*	g_2^*	u^*	$\tilde{v}^*$	g_3^*	w^*	a^*	$\lambda_1 \ldots \lambda_4$	λ_5	λ_6	λ_7
FP0	0	0	NF	NF	0	NF	NF	$(y<0,\varepsilon<0)$	$-\varepsilon$	0	0
FPI	0	0	NF	NF	$\frac{4}{3}\varepsilon$	0	$\frac{1}{2}$	$(y<0,\varepsilon<0)$	ε	$-\frac{1}{12}\varepsilon$	$\frac{1}{6}\varepsilon$
FPII	0	$\frac{8}{3}\varepsilon$	1	1	0	$w^*(a^*)$	$a^*(w^*)$	$(y<\frac{3}{2}\varepsilon,\varepsilon>0)$	$\Lambda_5(w^*)\varepsilon$	$\Lambda_6(w^*)\varepsilon$	0
FPIII	0	$\frac{8}{3}\varepsilon$	1	1	$0.3505(0)\varepsilon$	1.0819(3)	$\frac{1}{2}$	$(y<\frac{3}{2}\varepsilon,\varepsilon>0)$	$0.0438(1)\varepsilon$	$0.2165(3)\varepsilon$	$0.8083(8)\varepsilon$
FPIV	$G(\Delta)$	$H(\Delta)$	1	1	0	$w^*(a^*,\Delta)$	$a^*(w^*,\Delta)$	$(y>\frac{3}{2}\varepsilon,y>0)$	$\lambda_5(w^*,\Delta)$	$\lambda_6(w^*,\Delta)$	0
FPV	$G(\Delta)$	$H(\Delta)$	1	1	$g_3^*(\Delta)$	$w^*(\Delta)$	$\frac{1}{2}$	$(y>\frac{3}{2}\varepsilon,y>0)$	$\lambda_5(\Delta)$	$\lambda_6(\Delta)$	$\lambda_5(\Delta)$
$\underset{\alpha\to 0}{\text{FPIV}}$	$\frac{16}{9}y$	0	1	1	0	1	NF	$(y>\frac{3}{2}\varepsilon,y>0)$	$\frac{2}{3}(y-\frac{3}{2}\varepsilon)$	$\frac{1}{2}y$	0
$\underset{\alpha\to 0}{\text{FPV}}$	$\frac{16}{9}y$	0	1	1	$\frac{16}{15}(\frac{3}{2}\varepsilon-y)$	$\frac{1}{2}\left(\sqrt{1+\frac{40y}{4y-\varepsilon}}-1\right)$	$\frac{1}{2}$	$\left(y>\frac{3}{2}\varepsilon,y>0\right)$	$\lambda_5(y,\varepsilon)$	$\lambda_6(y,\varepsilon)$	$\frac{2}{15}(\frac{3}{2}\varepsilon-y)$
FPVI	0	$\frac{8}{3}\varepsilon$	∞	C	0	C	NF	Unstable	$-\frac{1}{3}\varepsilon$	$\frac{2(13+\sqrt{13})}{3(1+\sqrt{13})^2}\varepsilon$	0
FPVII	0	$\frac{8}{3}\varepsilon$	∞	C	$\frac{8}{15}\varepsilon$	$\frac{1}{6}(\sqrt{129}-3)$	$\frac{1}{2}$	Unstable	0.919918ε	0.295449ε	$\frac{1}{15}\varepsilon$
FPVIII	$\frac{8}{3}y$	0	∞	C	0	C	NF	Unstable	$\frac{2}{3}\left(y-\frac{3}{2}\varepsilon\right)$	$\frac{2(\sqrt{13}+13)}{3(\sqrt{13}+1)^2}y$	0
FPIX	$\frac{8}{3}y$	0	∞	C	$\frac{16}{15}(\frac{3}{2}\varepsilon-y)$	$\frac{1}{2}\left(\sqrt{1+\frac{40y}{4y-\varepsilon}}-1\right)$	$\frac{1}{2}$	Unstable	$\lambda_5(y,\varepsilon)$	$\lambda_6(y,\varepsilon)$	$\frac{2}{15}\left(\frac{3}{2}\varepsilon-y\right)$
FPX	Any from above				$\frac{4}{3}\varepsilon$	∞	$\frac{1}{2}$	Unstable			

IV. RESULTS

Since our model contains seven charges, in principle we can get up to approximately 2^7 universality classes. However, most of these fixed points do not exist due to the structure of beta functions. In a double expansion scheme (and in the case of models that contain nonuniversal parameters such as parameter α) we can also expect crossovers between different universality classes by varying these parameters.

A. Fixed points

Apart from the Gaussian (free) fixed point FP0, 11 fixed points have been found, out of which 4 embody qualitatively new universality classes. A list of all fixed points and eigenvalues of the corresponding stability matrix (75) is summarized in Table II.

(i) FP0: As expected, the trivial fixed point is stable for negative values of ε, y, and for any α.

(ii) FPI: The first nontrivial fixed point represents the bare DP process with an irrelevant velocity field, which corresponds to the standard DP regime [8,14]. In contrast to previous work [34,36], this fixed point has been found unstable to any permissible values of y,ε,α. We conclude that the effect of compressibility violates the stability of this fixed point.

(iii) FPII and FPII: These two fixed points correspond to universality classes of the passive scalar and DP advected by the thermal fluctuations of the velocity field. By a passive regime we henceforth have always in mind a regime for which DP interactions are irrelevant, i.e., $g_3^* = 0$. In these two cases, only a local part of the random force for velocity is relevant. For fixed point FPII with irrelevant DP interactions, we find that parameters w^* and a^* are not fixed. However, they are related to each other. Consequently, we do not have a fixed point, but rather a fixed line constrained by the relation $a^* = a^*(w^*)$. The plot of the function $w^*(a^*)$ can be seen in Fig. 4 and several explicit results together with eigenvalues of the stability matrix are given in Appendix C 2. If we restrict ourselves to the interval $a^* \in \langle 0,1\rangle$, parameter w^* attains values from the interval $\langle 1,1.0518(8)\rangle$ and the maximum value w^* is reached at $a^* = \frac{1}{2}$ (see Fig. 4). We have checked numerically that for any accessible value of $w^*(a^*)$ the eigenvalue λ_6 is negative for $\varepsilon > 0$, and therefore we infer that this fixed point is unstable. FPIII is stable in the region $y < 3\varepsilon/2$ and $\varepsilon > 0$.

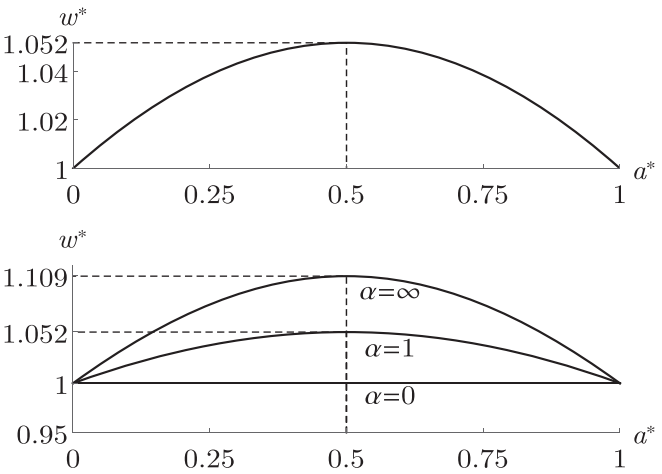

FIG. 4. Relation between w^* and a^* for FPII (upper figure) and FPIV (lower figure), respectively. For FPII, the parameter $w^* \in \langle 0,1.0518(8)\rangle$ for any $a^* \in \langle 0,1\rangle$. The same situation occurs in the case of FPIV, where the corresponding maximum depends on Δ. The lower plot is made for the physically relevant choice $(y,\varepsilon) = (4,1)$ and three different values of α. Note that all plots are symmetric around the point $a^* = \frac{1}{2}$.

In the case with $g_1^* > 0$ and $g_2^* > 0$, two fixed points have been found:

(i) FPIV: This regime describes turbulent advection of a passive scalar with irrelevant DP interactions. In a fashion similar to the fixed point FPII, parameters a^* and w^* cannot be determined unambiguously, but again they are related, and we have a whole line of fixed points. In contrast to FPII, this line depends on parameters $\Delta = \{y,\varepsilon,\alpha\}$. The explicit expression for $a^*(w^*)$ can be found in Appendix C 3. The plot for $(y,\varepsilon) = (4,1)$ and $\alpha \in \{0,1,\infty\}$ is shown in Fig. 4. For the purely longitudinal random forcing ($\alpha = 0$) we get $w^* = 1$, and parameter a^* remains undetermined. This is in accordance with results obtained in [61]. However, for $\alpha > 0$ we have $w^* > 1$ if $a^* \in \langle 0,1\rangle$. This means that the universality of the fixed point FPIV changes with $\alpha > 0$. Although it still corresponds to the turbulent advection by compressible turbulent flow, it is quantitatively different from that obtained in [61]. The plot for $\alpha > 0$ is symmetric around $a^* = \frac{1}{2}$ as in FPII with maxima at $w^* = 1.0518(8)$ for $\alpha = 1$ and $w^* = 1.1085(4)$ for $\alpha = \infty$.

(ii) FPV: The most nontrivial fixed point represents the universality class of DP advected by the compressible turbulent flow. In the case $\alpha = 0$, FPV becomes unstable for all (y,ε), and FPIV is stable for $y > 3\varepsilon/2$ and $\varepsilon > 0$. However, if $\alpha > 0$ the exact structure for $g_3^*(\Delta)$, $w^*(\Delta)$ as well as eigenvalues for FPV and FPIV are too cumbersome for a direct analysis. This problem requires a numerical solution of a complicated nonlinear set of connected differential equations [72].

Before we turn our attention to numerical results, let us discuss other analytical results. In order to obtain a full set of fixed points, one has to analyze limiting cases $\{u,v,w\} \to \infty$ as well. As can be easily seen from expressions (33) and (34), in the limit $u \to \infty$, the propagators $\langle v_i v_j\rangle_0$ and $\langle v_i v_j'\rangle_0$ become purely transversal, and the propagators $\langle v_i \phi_j\rangle_0$ and $\langle v_i \phi_j'\rangle_0$ vanish. Hence, $u \to \infty$ describes the incompressible limit. In this case, four fixed points FPVI-FPIX are found:

(i) FPVI and FPVII: These two fixed points describe new universality classes of a passive scalar and DP advected by thermal fluctuations of the incompressible velocity field. These two fixed points are not present in the previous studies, where the velocity field is generated by the incompressible NS equation [36]. The incompressible NS model does not possess divergence around $d = 4$, and therefore no fixed point with only g_2 relevant (in our notation) can appear.

(ii) FPVIII and FPIX: These two fixed points represent a universality class similar to FPVI and FPVII except that the velocity field now describes the fully developed incompressible turbulent flow. It can be shown that all fixed points of the velocity field in the incompressible limit are unstable [61].

The limiting case $\tilde{v} \to \infty$ is uninteresting since in the one-loop approximation the parameter $\tilde{v}$ enters only the $\beta_{\tilde{v}}$ function. Therefore, fixed-point values of other parameters are identical to the ones already mentioned above (see [61]). Similarly to the previous case, corresponding fixed points in the limit $u \to \infty$ are unstable.

Finally, let us discuss the limit $w \to \infty$. The contributions to the DP renormalization constants from the velocity field (terms proportional to g_1 and g_2) vanish, and accordingly the process belongs to the universality class of DP with irrelevant velocity field (see Appendix A). We have checked that for any fixed-point values for the velocity field the fixed point FPX is unstable for any Δ.

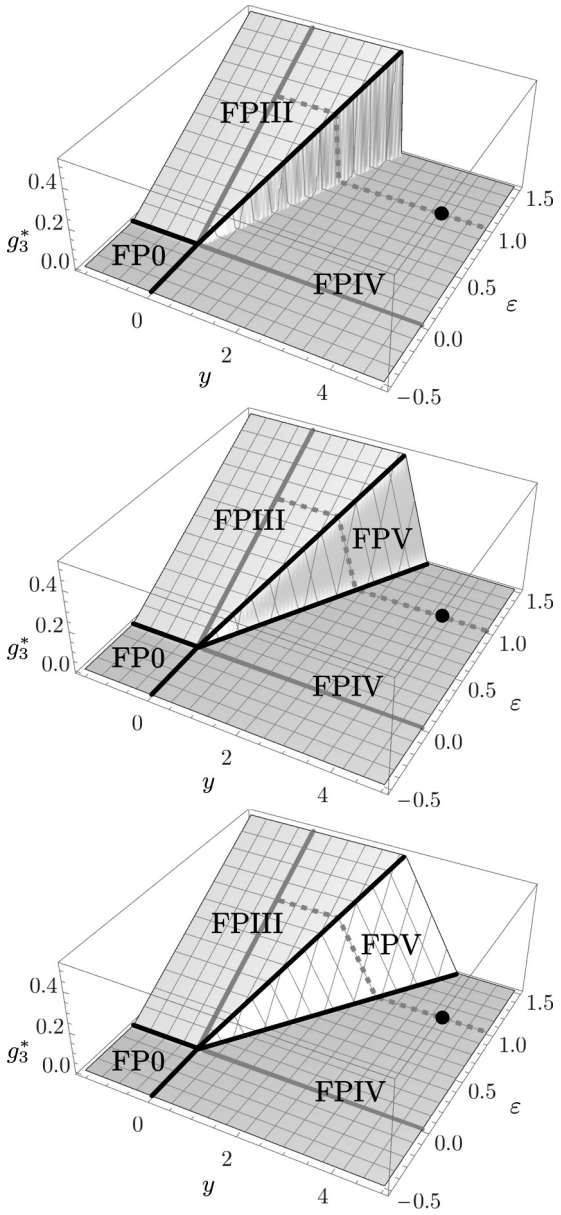

FIG. 5. Numerical solution for the fixed point's coordinate of the charge g_3^* for three different values of parameter $\alpha \in \{0,1,\infty\}$ (depicted in a given order from top to bottom). Distinct regions of stability are separated by the solid black line, the line $\varepsilon = 1$ ($d = 3$) is represented by the gray dashed line, and black dot represents the case $(y,\varepsilon) = (4,1)$. Technical details concerning boundary between regions of stability for FPIV and FPV can be found in Appendix C 5.

Numerical verification. To confirm the restricted picture obtained in an analytical fashion, we have numerically sought fixed-point solutions of β functions. Results for the coupling constant g_3^* in the (y,ε) plane for three different values of parameter α are shown in Fig. 5. These RG flows are calculated with initial conditions $(g_1,g_2,u,v) = (1,1,1,1)$ for the cNS charges. Varying initial conditions might, of course, change the structure of the RG flow, but the universal quantities have to remain unchanged (for positive initial values). In the case

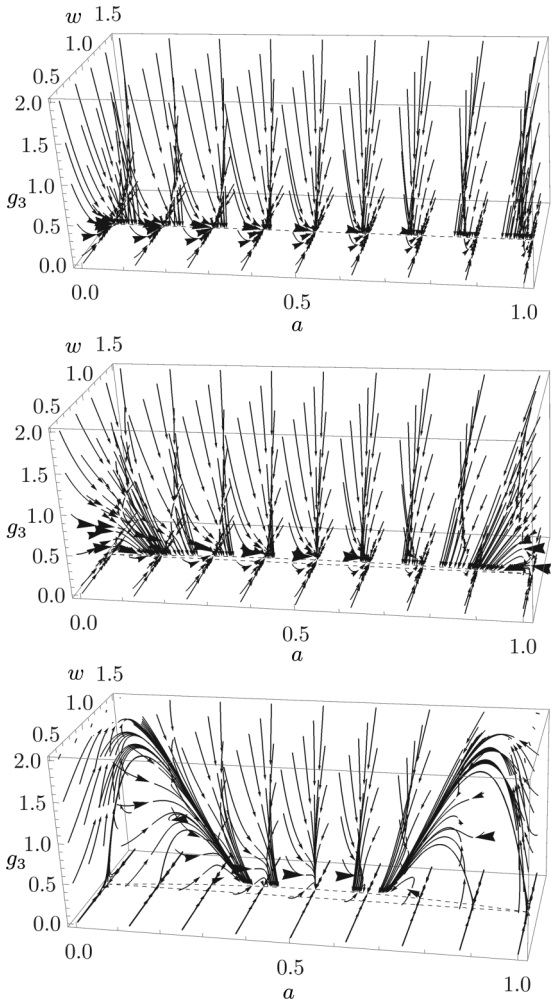

FIG. 6. RG flow in the (a,w,g_3) plane for the physical values $(y,\varepsilon)=(4,1)$ and for $\alpha\in\{0,1,\infty\}$ (from top to bottom). By increasing the value of α, the fixed (dashed) line shifts from $w=1$.

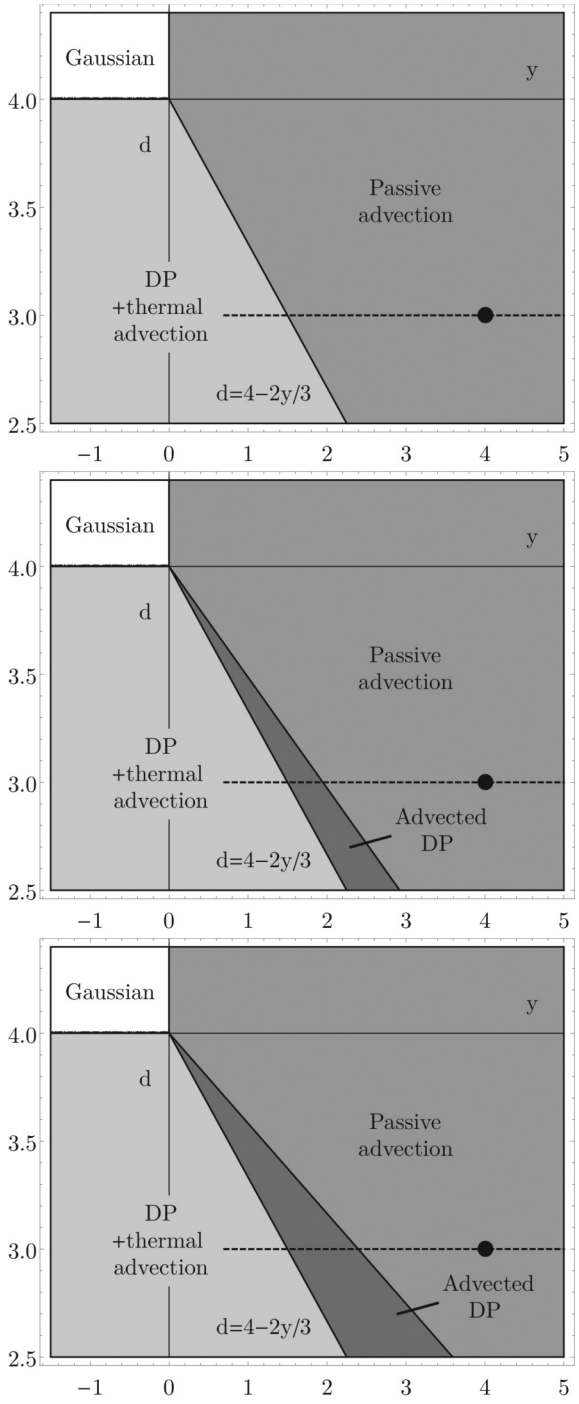

FIG. 7. Phase portraits in the (d,y) plane for the values $\alpha\in\{0,1,\infty\}$ (from top to bottom). For $\alpha>0$, four regimes are present and in the limit $\alpha\to 0$ advected DP regime vanishes. The case $d=3\,(\varepsilon=1)$ is denoted with the dashed line, so that the crossover with growing α between distinct regimes is clearly visible. The most relevant point $(d,y)=(3,4)$ (denoted by the black dot) belongs to the universality class of passive advection.

of purely transversal random force $\alpha=0$, only three stable fixed points have been found, FP0, FPII and FPIV, which is in accordance with our analytical results. For the physically relevant values $(y,\varepsilon)=(4,1)$ the system belongs to the universality class of passive scalar advected by the compressible turbulent flow. By increasing the value of α, the existence of another fixed point FPV emerges. The region of stability for FPV gets larger with an increasing α. In the limit $\alpha\to\infty$ (pure longitudinal random force scenario), the boundary between FPIV and FPV does not cross the physical point $(y,\varepsilon)=(4,1)$. Therefore, we do not observe any crossover between universality classes by changing the structure of the velocity field random force. A numerical calculation of the RG flow for the physical values of parameters $(y,\varepsilon)=(4,1)$ can be seen in Fig. 6. We have again performed a calculation for three different values of α. For $\alpha=0$ one immediately observes that there is an entire line of fixed points with $g_3^*=0$, $w^*=1$, and a^* not fixed (dashed line). Moreover, the RG flow is symmetric around the plane $a^*=\frac{1}{2}$, and the further from the center the flow begins, the more attracted towards the center it is. The larger value α takes, the stronger attraction is observed. This can be particularly seen in the case of $\alpha=1$. In addition, the line of fixed points shifts away from the former line to $w^*=w^*(a^*)$. In the limit $\alpha\to\infty$, even the stability of this line changes, so that regions around $a^*=0$ and $a^*=1$ become unstable.

Phase portrait. For convenience, we have constructed a schematic phase portrait with regions of stability in Fig. 7 in

TABLE III. Anomalous dimensions and critical exponents for various fixed points with shorthand notation $\Delta = \{y,\varepsilon,\alpha\}$. Some gamma functions are not displayed due to their cumbersome structure. Nonuniversality affects only anomalous dimensions for DP fields and critical exponents that originate from them. Exponents δ and δ' differ only if the nonuniversality is present for $a^* \neq \frac{1}{2}$. Corresponding values for fixed point FPX are not displayed since they are identical to FPI.

FP/γ^*|exp	$\gamma_\psi^*,\gamma_{\psi'}^*$	γ_τ^*	γ_D^*	$\tilde{z}$	Θ	δ, δ'
FP0	0	0	0	1	0	$1-\frac{1}{4}\varepsilon$
FPI	$-\frac{1}{12}\varepsilon$	$-\frac{1}{4}\varepsilon$	$\frac{1}{12}\varepsilon$	$1+\frac{1}{14}\varepsilon$	$\frac{1}{12}\varepsilon$	$1-\frac{1}{4}\varepsilon$
FPII	$\gamma_\psi(a^*,\varepsilon) \neq \gamma_{\psi'}(a^*,\varepsilon)$	$-\frac{1}{2}\varepsilon$	$\frac{1}{2}\varepsilon$	$1+\frac{1}{4}\varepsilon$	$T(a^*)\varepsilon$	$1-\frac{\gamma_\psi(a^*,\varepsilon)}{2} \neq 1-\frac{\gamma_{\psi'}(a^*,\varepsilon)}{2}$
FPIII	$-0.0603(6)\varepsilon$	$-0.5438(1)\varepsilon$	$\frac{1}{2}\varepsilon$	$1+0.0109(5)\varepsilon$	$0.0219(1)\varepsilon$	$1-\frac{1}{4}\varepsilon$
FPIV	$\gamma_\psi^*(a^*,\Delta) \neq \gamma_{\psi'}^*(a^*,\Delta)$	$-\frac{1}{3}y$	$\frac{1}{3}y$	$\frac{2}{2-y/3}$	$\Theta(a^*,\Delta)$	$\delta(a^*,\Delta) \neq \delta'(a^*,\Delta)$
FPV	$\gamma_\psi^*(\Delta) = \gamma_{\psi'}^*(\Delta)$	$-\frac{1}{3}y+\frac{1}{8}g_3^*(\Delta)$	$\frac{1}{3}y$	$\frac{2}{2-y/3}$	$\Theta(\Delta)$	$\delta(\Delta) = \delta'(\Delta)$
FPIV $\alpha\to 0$	0	$-\frac{1}{3}y$	$\frac{1}{3}y$	$\frac{2}{2-y/3}$	0	$\frac{4-\varepsilon}{2(2-y/3)}$
FPV $\alpha\to 0$	$\frac{1}{30}(2y-3\varepsilon)$	$-\frac{1}{5}(y+\varepsilon)$	$\frac{1}{3}y$	$\frac{2}{2-y/3}$	$-\frac{3(2y-3\varepsilon)}{5(2-y/3)}$	$\frac{30+y-9\epsilon}{15(2-y/3)}$
FPVI	0	$-\frac{1}{3}\varepsilon$	$\frac{1}{3}\varepsilon$	$1+\frac{1}{6}\varepsilon$	0	$1-\frac{1}{12}\varepsilon$
FPVII	$-\frac{1}{30}\varepsilon$	$-\frac{2}{5}\varepsilon$	$\frac{1}{3}\varepsilon$	$1+\frac{1}{6}\varepsilon$	$\frac{1}{30}\varepsilon$	$1-\frac{1}{10}\varepsilon$
FPVIII	0	$-\frac{1}{3}y$	$\frac{1}{3}y$	$\frac{2}{2-y/3}$	0	$\frac{4-\varepsilon}{2(2-y/3)}$
FPIX	$\frac{1}{30}(2y-3\varepsilon)$	$-\frac{1}{5}(y+\varepsilon)$	$\frac{1}{3}y$	$\frac{2}{2-y/3}$	$-\frac{3(2y-3\varepsilon)}{5(2-y/3)}$	$\frac{30+y-9\epsilon}{15(2-y/3)}$

the (d,y) plane. Different regions of stability are denoted by different shades of gray. For the physical values of parameters $(d,y) = (3,4)$ the system lies within the regime of the passive scalar advected by the compressible turbulent flow, where DP interactions are irrelevant. This phase portrait possesses a few differences from results obtained by previous authors. In [34,36], it was established that in the case of incompressible turbulence for the physical values of parameters, the model should belong to the universality class of passive advection and DP is effectively irrelevant. With the account of the effect of compressibility, the region of stability for an advected DP expands and above a certain level of compressibility DP interactions become relevant. This difference might be traced to the fact that in the present model the parameter α, which is responsible for the quantitative change of the phase portrait, does not generally describe the level of compressibility. Further, in the previous work [67,73] the parameter α (in their notation) has to fulfill a certain condition involving scaling parameter of the velocity field.

B. Critical scaling

In this section, we discuss universal scaling properties of the DP process advected by the fully developed compressible turbulent flow. At the critical point, the total scaling dimension of any quantity Q is given by the relation [5,7]

$$\Delta_Q = d_Q^k + \Delta_\omega d_Q^\omega + \gamma_Q^*, \quad \Delta_\omega = 2 - \gamma_D^*, \tag{76}$$

where $\gamma_Q^* = \gamma_Q(g^*)$ is a fixed-point value. Applying a scaling analysis on definitions (10)–(13) we get the following expressions for critical exponents [8,58]:

$$\Theta = -\frac{\gamma_\psi^* + \gamma_{\psi'}^*}{\Delta_\omega}, \quad \tilde{z} = \frac{2}{\Delta_\omega}, \tag{77}$$

$$\delta = \frac{d/2 + \gamma_\psi^*}{\Delta_\omega}, \quad \delta' = \frac{d/2 + \gamma_{\psi'}^*}{\Delta_\omega}. \tag{78}$$

Anomalous dimensions and critical exponents of the model under consideration can be seen in Table III. A few analytical expressions are too lengthy, so they are not displayed explicitly.

Nonuniversality. Let us first begin by discussing a presence of nonuniversality. It has turned out that the anomalous dimensions γ_τ^* and γ_D^* are independent of charges $a^*(w^*)$ in the case of all fixed points (see Appendix C 1). As a result, the nonuniversality shows up only in anomalous dimensions γ_ψ and $\gamma_{\psi'}$ for regimes FPII and FPIV. The only exception is FPV, where γ_τ^* depends on α. It should also be emphasized that the result $\gamma_D^* = y/3$ for regimes FPIV, FPV, FPVIII, FPIX and $\gamma_\tau^* = -y/3$ for regimes FPIV, FPVIII are in fact exact results. This follows from the fact that in these cases γ_D^* and γ_τ^* are calculated solely from γ_ν^* which is known exactly due to nonrenormalizability of the nonlocal part of the random force correlator (27) [7,61].

Although the rapidity symmetry (17) is generally broken, critical exponents describing density of species δ and the survival probability δ' are identical if DP is relevant (FPI, FPIII, FPV). This is because anomalous dimensions for DP fields possess the following symmetry:

$$\gamma_\psi(a) = \gamma_{\psi'}(1-a), \tag{79}$$

and so they are equal for $a^* = \frac{1}{2}$ [see Eqs. (B6) and (B7)]. However, if the DP is irrelevant (FPII, FPIV) the parameter a^* does not necessarily reach the fixed-point value $a^* = \frac{1}{2}$. The region of stability as well as the final value of a^* then depends on its initial value a in the RG flow and on parameters Δ as it has been shown in Fig. 6. For any other fixed-point value than $a^* = \frac{1}{2}$, critical exponents δ and δ' differ. Scaling properties of the Gaussian and DP fixed points (FP0, FPI) are in agreement with [14]. Results of FPII and FPIII universality class have not been obtained before, but these fixed points are unstable. The critical exponents Θ, δ, and δ' for FPII are depicted in Fig. 8. The critical exponent Θ is symmetric around $a^* = \frac{1}{2}$ and exponents δ and δ' are symmetric within each other with respect to $a^* = \frac{1}{2}$.

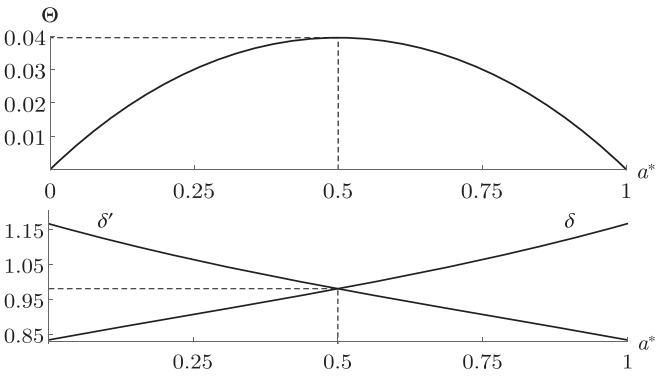

FIG. 8. Critical exponents for FPII for $\varepsilon = 1$ as a function of a^*.

The final expressions of $\tilde{z}$ for regimes FPIV and FPV are exact. Note that in [34] authors do not normalize the definition for $\mathcal{R}$ with the expression $\mathcal{N}$. As a result, a different exponent $\tilde{z}$ is obtained. For the physical value of parameter $y = 4$ we obtain $R^2 \sim t^3$ which is in agreement with the Richardson's law $dR^2/dt \sim R^{4/3}$ for turbulent diffusion [31,40]. Explicit results for other exponents and anomalous dimensions are in the case of FPIV and FPV too lengthy for an analytical analysis. We discuss a numerical calculation of critical exponents later.

Scaling properties of the first two universality classes in the incompressible limit (FPVI, FPVII) have not been found in the previous work [36]. This is due to the fact that the incompressible model of NS turbulence does not possess divergence around $d = 4$ and therefore a fixed point determined solely by g_2 (in our notation) does not exist. The results of the other two universality classes in the incompressible limit (FPVIII, FPIX) are in agreement with the results obtained in [36].

A very intriguing result is that the universality class of the passive scalar and DP advected by the compressible turbulent flow (FPIV,FPV) coalesces with the incompressible limit for $\alpha \to 0$. The reason for this result may be related to the fact that in the limit $\alpha \to 0$, the model (30) for the fully developed compressible turbulence shows an incompressible Kolmogorov $-\frac{5}{3}$ energy spectrum [60].

Numerical solution of critical exponents. We have computed critical exponents numerically for the physically relevant choice $(y,\varepsilon) = (4,1)$ as a function of α and the initial value a in the RG flow. The result for exponents Θ, δ and the difference $\Delta\delta = |\delta - \delta'|$ are displayed in Fig. 9. It is noticeable that the limit $\alpha \to 0$ converges to the incompressible case and the results are universal, i.e., independent of the initial value a. For $a = \frac{1}{2}$ we do not observe any substantial change of δ or $\Delta\delta$ as a function of α. By increasing α, a nonuniversality with respect to the initial value a emerges. The more a deviates from $a = \frac{1}{2}$, the faster increase of δ and $\Delta\delta$ as function of α, mainly in region $\alpha \gtrsim 1$. A similar situation is observed in other stochastic models, e.g., in case of the stochastic magnetohydrodynamic turbulence [74], where the decisive role is played by a forcing decay parameter.

An increase of the value of the parameter α also drastically changes values of critical exponents. The exponent Θ shows a rapid increase for $\alpha \gtrapprox 1$, while exponents δ and δ' show very weak dependence for $\alpha \lessapprox 1$. Moreover, we observe a certain degree of symmetry in critical exponents. For instance, the exponent describing a number of particles Θ is symmetric

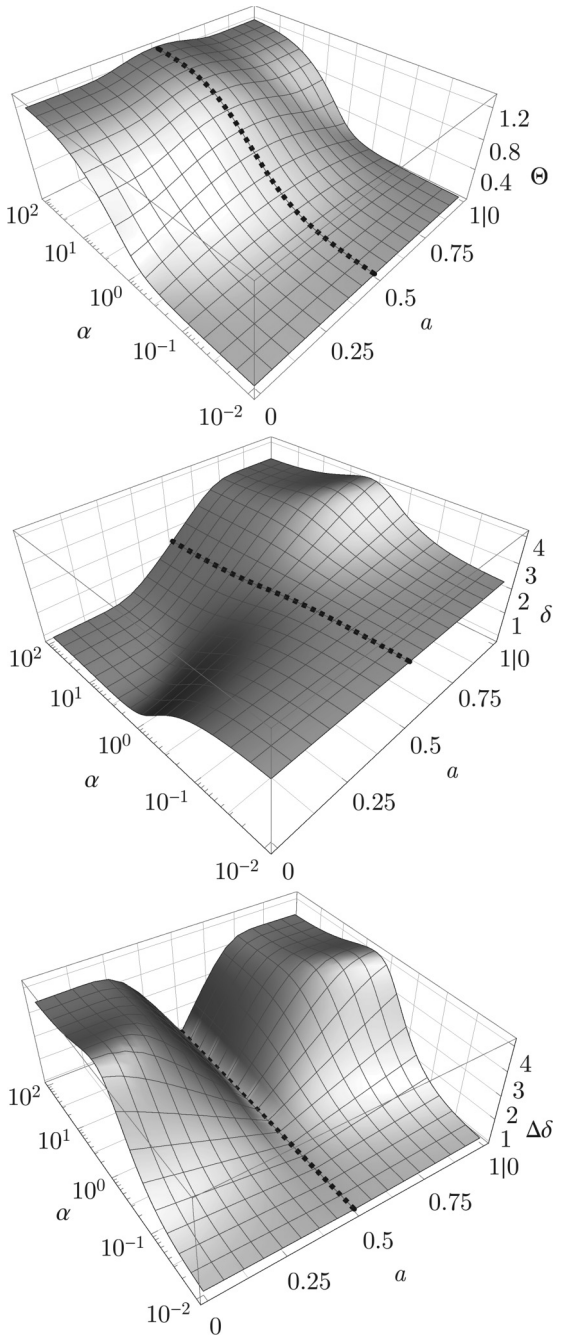

FIG. 9. Numerical solution for critical exponents Θ, δ and the difference $\Delta\delta = |\delta - \delta'|$ (from top to the bottom). Result for the exponent δ' is horizontally symmetric to δ with respect to the plane $a = \frac{1}{2}$ (not displayed). For $\alpha \to 0$ exponents tend to the incompressible limit and the difference $\Delta\delta$ vanishes.

with respect to the transformation $a \leftrightarrow 1 - a$, i.e., symmetric around $a = \frac{1}{2}$. The graph for δ' is horizontally symmetric to δ with respect to the $a = \frac{1}{2}$ plane. This is due to the symmetry (79), which follows from the fact that renormalization constants are symmetric with respect to the transformation

$$Z_i(a) = Z_i(1-a) \quad \text{for } i = 1,2,3, \tag{80}$$

$$Z_4(a) = Z_5(1-a), \tag{81}$$

$$Z_1(a) - aZ_6(a) = (1-a)Z_6(1-a). \tag{82}$$

The above symmetry was proposed in [58] as a result of the time-reversal symmetry of the compressible Kraichnan-velocity ensemble. It is unclear whether relations (80)–(82) hold also in the present case since the cNS model (30) is not time-reversal invariant. A broken time-reversal invariance by the incompressible NS velocity ensemble has not been discussed in [36], although the authors obtained the same anomalous dimensions γ_ψ and $\gamma_{\psi'}$.

V. CONCLUSIONS

In this paper, we have analyzed the critical behavior of the DP process in the presence of the velocity fluctuations of an ambient environment. We have shown how to construct a functional representation of the problem. We have demonstrated that the model is multiplicatively renormalizable, which ensures utilization of methods of the field-theoretic renormalization group to obtain relevant information about the large-scale and long-time behavior of the model. Depending on the dimensionality of the space d, the scaling exponent y of the velocity field, and pumping parameter α, we have found 11 universality classes, out of which only 4 classes have IR stable fixed points and thus are macroscopically relevant. In contrast to previous works [58,68], the compressibility is present in the model at all stages. The parameter α plays a special role, which is associated with the pumping of longitudinal modes into the velocity flow.

Compressibility changes stability of certain regimes, which can be deduced from the fixed-point structure. The pure DP regime of FPI becomes unstable and is effectively replaced by the regime of FPIII with the combined effect of DP interactions and local stirring of the velocity field. We observe that the mutual interplay between the nonlinear DP interactions and advection in the compressible flow gives rise to a nontrivial regime of FPV. Further, we see that the larger the input of compressible modes, the larger the stability region. Compressible modes thus enhance stabilization of the DP nonlinearities. We have also estimated that the effect is not strong enough to affect the physically relevant three-dimensional turbulent case.

From a numerical analysis of the critical exponents, we have obtained additional consequences. First, we see that the parameter α has direct influence on the value of some critical exponents (see FPIV and FPV in Table II). The spreading exponent $\tilde{z}$ is not affected by α at all and for all fixed points it is expressed in terms of the universal quantities ε and y. We have analyzed the incompressible limit $u \to \infty$ and the limit $v \to \infty$, and the results are in agreement with previously obtained results. Nonuniversality is especially pronounced in the physically most relevant three-dimensional ($d = 3$) case with $y = 4$. There, an enhancement of the DP process is exhibited in the behavior of the exponent Θ (see Figs. 8 and 9). Although α does not affect the stability of FPV, it does affect the critical exponents quite heavily. This fact can be explained by the presence of compressible sinks into which particles are attracted [75].

Future studies should involve higher-order loop calculations to confirm the physical picture we have presented here. Moreover, there are interesting questions regarding possible influence of the percolation process on the velocity field. Work on these topics is in progress.

ACKNOWLEDGMENTS

The authors thank P. Muratore-Ginanneschi, D. Mitra, and M. Hnatič for many illuminating and fruitful discussions. The work was supported by VEGA Grant No. 1/0345/17 of the Ministry of Education, Science, Research and Sport of the Slovak Republic by the Ministry of Education and Science of the Russian Federation (the Agreement No. 02.a03.21.0008), the grant of the Slovak Research and Development Agency under the Contract No. APVV-16-0186. The authors are indebted to Zuzana and Peter Bodík and N. M. Gulitskiy for critical reading of the manuscript, and H. Bänsch for a help with a preparation of figures.

APPENDIX A: RENORMALIZATION CONSTANTS

1. Self-energy diagram

In this appendix, we give an explicit example of a typical calculation of the Feynman diagram. Let us consider the self-energy diagram

$I =$  . (A1)

We choose an external momentum $p = (\boldsymbol{p}, \Omega)$ to flow through the lower propagator $\langle \psi \psi' \rangle_0$ and the internal momentum $k = (\boldsymbol{k}, \omega)$ flows clockwise in the loop. Using the standard Feynman diagrammatic technique based on Eqs. (33)–(44), we construct the following algebraic expression for the diagram

$$I(p) = \int \frac{d^d k}{(2\pi)^d} \int \frac{d\omega}{2\pi} V_{\psi' v_1(-\boldsymbol{k})\psi(\boldsymbol{k}-\boldsymbol{p})} \langle \psi \psi' \rangle_0 (p-k) \times V_{\psi' v_2(\boldsymbol{k})\psi(\boldsymbol{p}-\boldsymbol{k})} \langle v_1 v_2 \rangle_0 (k), \quad \text{(A2)}$$

or in a detailed explicit form

$$I = (-i)^2 \int \frac{d^d k}{(2\pi)^d} \int \frac{d\omega}{2\pi} \frac{-[(p-k)_1 + ak_1](ak_2 - p_2)}{L(p-k)} \times \left(P_{12}(\boldsymbol{k}) \frac{d_1^f(\boldsymbol{k})}{|\epsilon_1(k)|^2} + Q_{12}(\boldsymbol{k}) d_2^f(\boldsymbol{k}) \left| \frac{\epsilon_3(k)}{R(k)} \right|^2 \right). \quad \text{(A3)}$$

First of all, let us note that the correction to the vertex function $\Gamma^{\psi\psi'}$ is independent of c_0 and therefore we may set $c_0 = 0$ in the above expression. Expanding the terms in brackets, the calculation is effectively divided in an evaluation of two integrals $I = I_P + I_Q$:

$$I_P = \int \frac{d^d k}{(2\pi)^d} \int \frac{d\omega}{2\pi} \frac{T_{12}(\boldsymbol{p},\boldsymbol{k}) P_{12}(\boldsymbol{k}) d_1^f(\boldsymbol{k})}{L(p-k)|\epsilon_1(k)|^2}, \quad \text{(A4)}$$

$$I_Q = \int \frac{d^d k}{(2\pi)^d} \int \frac{d\omega}{2\pi} \frac{T_{12}(\boldsymbol{p},\boldsymbol{k}) Q_{12}(\boldsymbol{k}) d_2^f(\boldsymbol{k})}{L(p-k)|\epsilon_2(k)|^2}, \quad \text{(A5)}$$

where we have introduced $T_{12}(\boldsymbol{p},\boldsymbol{k}) = [(p-k)_1 + ak_1](ak_2 - p_2)$. Let us first calculate the I_P part. The calculation of the tensor structure yields

$$P_{12}(\boldsymbol{k}) T_{12}(\boldsymbol{p},\boldsymbol{k}) = \left(\frac{(\boldsymbol{p}\cdot\boldsymbol{k})^2}{k^2} - p^2 \right). \quad \text{(A6)}$$

Since the tensor structure is already proportional to p^2, we can set $\boldsymbol{p} = \Omega = \tau = 0$ in the rest of the calculation. The next step

is to perform the frequency integration

$$\int \frac{d\omega}{2\pi} \frac{1}{L(-k)|\epsilon_1(k)|^2} = \frac{1}{2(1+w_0)v_0^2 k^4}. \tag{A7}$$

Then, the expression I_P part is equal to

$$I_P = \frac{1}{2(1+w_0)v_0^2} \int \frac{d^d k}{(2\pi)^d} \left(\frac{(\boldsymbol{p}\cdot\boldsymbol{k})^2}{k^2} - p^2 \right) \frac{d_1^f(\boldsymbol{k})}{k^4}. \tag{A8}$$

In order to carry out the momentum integration, we need the following formula for isotropic integrals:

$$\int d^d k\, k_i k_j f(k^2) = \frac{1}{d} \int d^d k\, k^2 f(k^2) \tag{A9}$$

that allows us to perform a valid substitution $(\boldsymbol{p}\cdot\boldsymbol{k})^2 \to p^2 k^2/d$ in Eq. (A6). We are thus left with simple d-dimensional integrals of two types

$$\int_m^\infty \frac{d^d k}{(2\pi)^d} \frac{k^{4-d-y}}{k^4} = \overline{S_d} \frac{m^{-y}}{y}, \tag{A10}$$

$$\int_m^\infty \frac{d^d k}{(2\pi)^d} \frac{1}{k^4} = \overline{S_d} \frac{m^{-\varepsilon}}{\varepsilon}, \tag{A11}$$

where $\overline{S_d} \equiv S_d/(2\pi)^d$ and $S_d = 2\pi^{d/2}/\Gamma(d/2)$ is the surface of a d-dimensional sphere. The final result then reads as

$$\frac{I_P}{D_0 p^2} = \frac{(1-d)\overline{S_d}}{2w_0(1+w_0)d} \left(\frac{g_{10} m^{-y}}{y} + \frac{g_{20} m^{-\varepsilon}}{\varepsilon} \right). \tag{A12}$$

In a similar way, the tensor structure of the I_Q part yields

$$Q_{12}(\boldsymbol{k}) T_{12}(\boldsymbol{p},\boldsymbol{k}) = a_0(a_0-1)k^2 + (\boldsymbol{p}\cdot\boldsymbol{k}) - \frac{(\boldsymbol{p}\cdot\boldsymbol{k})^2}{k^2}, \tag{A13}$$

and the frequency integration gives

$$\begin{aligned} &\int \frac{d\omega}{2\pi} \frac{1}{L(-k)|\epsilon_2(k)|^2} \\ &\approx \frac{1}{2u_0(u_0+w_0)v_0^2 k^4} \\ &\quad \times \left(1 + \frac{i\Omega + w_0[2(\boldsymbol{p}\cdot\boldsymbol{k}) - p^2 - \tau_0]}{(u_0+w_0)k^2} + \frac{4w_0^2(\boldsymbol{p}\cdot\boldsymbol{k})^2}{(u_0+w_0)^2 k^4} \right), \end{aligned} \tag{A14}$$

where we have already performed the Taylor expansion to the first order in variables Ω, τ_0, and to the second order in the external momentum $\boldsymbol{p}$. Multiplying expressions (A13) and (A14), keeping only terms proportional to Ω, p^2, and τ_0 and integrating over the momentum $\boldsymbol{k}$, we finally obtain

$$\begin{aligned} I_Q = {} & \frac{\overline{S}_d}{2u_0(u_0+w_0)^2} \left(g_{10}\alpha \frac{m^{-y}}{y} + g_{20} \frac{m^{-\varepsilon}}{\varepsilon} \right) \\ & \times \left\{ p^2 D_0 \left[\frac{w_0 - u_0}{d w_0} + \frac{a_0(a_0-1)w_0}{(u_0+w_0)} \left(\frac{4}{d} - \frac{u_0}{w_0} - 1 \right) \right] \right. \\ & \left. + a_0(a_0-1)(i\Omega - \tau_0 D_0) \right\}. \end{aligned} \tag{A15}$$

2. Renormalization constants

Calculation shows that the general structure of the renormalization constants for the current model in the one-loop approximation can be written as follows:

$$Z_i = 1 + z_1^{(i)}(r)\frac{g_1}{y} + z_2^{(i)}(r)\frac{g_2}{\varepsilon} + z_3^{(i)}(r)\frac{g_3}{\varepsilon}, \tag{A16}$$

where $r = \{u, v, w, a\}$ and all coefficient functions z_i in (A16) are analytic functions of the regulators ε and y. It is convenient to express contributions of the type (A15) in the form of functions of renormalized parameters with the use of relations (54)–(56). For simplicity, we adopt the normalization-point scheme with the choice $\mu/m = 1$ and calculate the coefficient functions z_i in (A16) only at the leading order of expansion in ε and y. The resulting renormalization constants for the DP process are

$$Z_1 = 1 + \frac{a(1-a)}{2u(u+w)^2} G_1 + \frac{g_3}{8\varepsilon}, \tag{A17}$$

$$\begin{aligned} Z_2 = {} & 1 + \frac{(1-d)}{2w(1+w)d} G_2 + \frac{1}{2u(u+w)^2} \left[\frac{w-u}{dw} \right. \\ & \left. + \frac{a(a-1)w}{u+w} \left(\frac{4}{d} - \frac{u}{w} - 1 \right) \right] G_1 + \frac{d-2}{8d} \frac{g_3}{\varepsilon}, \end{aligned} \tag{A18}$$

$$Z_3 = 1 - \frac{a(a-1)}{2u(u+w)^2} G_1 + \frac{g_3}{4\varepsilon}, \tag{A19}$$

$$Z_4 = 1 - \left(\frac{(1-a)^2}{2uw(u+w)} + \frac{a(a-1)}{u(u+w)^2} \right) G_1 + \frac{g_3}{2\varepsilon}, \tag{A20}$$

$$Z_5 = 1 - \left(\frac{a^2}{2uw(u+w)} + \frac{a(a-1)}{u(u+w)^2} \right) G_1 + \frac{g_3}{2\varepsilon}, \tag{A21}$$

$$Z_6 = 1 + \frac{a(1-a)}{2u(u+w)^2} G_1 + \frac{d(d-1)+3}{4ad} \frac{g_3}{\varepsilon}, \tag{A22}$$

where we have introduced

$$G_1 = \left(\frac{\alpha g_1}{y} + \frac{g_2}{\varepsilon} \right), \quad G_2 = \left(\frac{g_1}{y} + \frac{g_2}{\varepsilon} \right). \tag{A23}$$

The remaining Feynman diagrams can be analyzed in a similar fashion.

APPENDIX B: RG FUNCTIONS

1. Anomalous dimensions

Anomalous dimensions are found from the renormalization constants in the following way. From Eqs. (68) and (A16) the general form of the anomalous dimensions at the one-loop order readily follows:

$$\gamma_i = -z_i^{(1)}(r) g_1 - z_i^{(2)}(r) g_2 - z_i^{(3)}(r) g_3 . \tag{B1}$$

Relations between anomalous dimensions are found from Eqs. (59)–(61):

$$\gamma_\psi = (\gamma_1 + \gamma_5 - \gamma_4)/2, \quad \gamma_D = \gamma_2 - \gamma_1, \tag{B2}$$

$$\gamma_{\psi'} = (\gamma_1 - \gamma_5 + \gamma_4)/2, \quad \gamma_\tau = \gamma_3 - \gamma_2, \tag{B3}$$

$$\gamma_\lambda = (\gamma_4 + \gamma_5 - \gamma_1)/2 - \gamma_2, \quad \gamma_{g_3} = 2\gamma_\lambda, \tag{B4}$$

$$\gamma_w = \gamma_D - \gamma_v = \gamma_2 - \gamma_1 - \gamma_v, \quad \gamma_a = \gamma_6 - \gamma_1. \tag{B5}$$

The final form of the anomalous dimensions is

$$\gamma_\psi = \left(\frac{(a-1)a}{2u(u+w)^2} + \frac{2a-1}{2uw(u+w)}\right)(\alpha g_1 + g_2) - \frac{g_3}{8}, \tag{B6}$$

$$\gamma_{\psi'} = \left(\frac{(a-1)a}{2u(u+w)^2} + \frac{1-2a}{2uw(u+w)}\right)(\alpha g_1 + g_2) - \frac{g_3}{8}, \tag{B7}$$

$$\gamma_{g_3} = (\alpha g_1 + g_2)\left(\frac{3(a-1)a}{2u(u+w)^2} + \frac{2(a-1)a+1}{2uw(u+w)} - \frac{4(a-1)auw + u^2 - w^2}{4uw(u+w)^3}\right) - \frac{3(g_1+g_2)}{4w(w+1)} - \frac{3g_3}{4}, \tag{B8}$$

$$\gamma_\tau = \frac{[(1-2a)^2w^2 - u^2]}{8uw(u+w)^3}(\alpha g_1 + g_2) - \frac{3(g_1+g_2)}{8w(w+1)} - \frac{3g_3}{16}, \tag{B9}$$

$$\gamma_D = \frac{[u^2 - (1-2a)^2w^2]}{8uw(u+w)^3}(\alpha g_1 + g_2) + \frac{3(g_1+g_2)}{8w(w+1)} + \frac{g_3}{16}, \tag{B10}$$

$$\gamma_\nu = \frac{(u-1)}{8u(u+1)^2}(\alpha g_1 + g_2) + \frac{(3u^2+8u+7)}{24(u+1)^2}(g_1+g_2), \tag{B11}$$

$$\gamma_w = \left(\frac{u^2 - (1-2a)^2w^2}{8uw(u+w)^3} + \frac{1-u}{8u(u+1)^2}\right)(\alpha g_1 + g_2) + \left(\frac{3}{8w(w+1)} - \frac{3u^2+8u+7}{24(u+1)^2}\right)(g_1+g_2) + \frac{g_3}{16}, \tag{B12}$$

$$\gamma_a = \frac{(1-2a)g_3}{16a}, \tag{B13}$$

where we have included γ_ν for completeness [61].

2. Beta functions

The β functions, which express RG flow, are easily found from Eq. (72):

$$\beta_{g_3} = -g_3\left[\varepsilon + \left(\frac{3(a-1)a}{2u(u+w)^2} + \frac{2(a-1)a+1}{2uw(u+w)} - \frac{4(a-1)auw + u^2 - w^2}{4uw(u+w)^3}\right)(\alpha g_1 + g_2) - \frac{3(g_1+g_2)}{4w(w+1)} - \frac{3g_3}{4}\right], \tag{B14}$$

$$\beta_w = -w\left[\left(\frac{u^2 - (1-2a)^2w^2}{8uw(u+w)^3} + \frac{1-u}{8u(u+1)^2}\right)(\alpha g_1 + g_2) + \left(\frac{3}{8w(w+1)} - \frac{3u^2+8u+7}{24(u+1)^2}\right)(g_1+g_2) + \frac{g_3}{16}\right], \tag{B15}$$

$$\beta_a = g_3\frac{2a-1}{16}. \tag{B16}$$

APPENDIX C: EXPLICIT EXPRESSIONS

1. Universality of anomalous dimensions γ_τ^* and γ_D^*

Let us consider a fixed point with $\gamma_w^* = 0$ and $w^* \neq 0$. Using relations (B2)–(B5) we derive

$$\gamma_\tau^* = -\gamma_\nu^* + \gamma_3^* - \gamma_1^* = -\gamma_\nu^* - \frac{g_3^*}{8}, \quad \gamma_D^* = \gamma_\nu^*. \tag{C1}$$

We have seen that γ_ν^* is independent of $a^*(w^*)$ [see Eq. (B11)]. Relations (C1) then imply that anomalous dimensions γ_τ^* and γ_D^* are unaffected by the nonuniversality in $a^*(w^*)$ appearing for fixed points FPII and FPIV. In the case of FPI with $w^* = 0$ anomalous dimensions (B9) and (B10) are independent of a^*. To avoid possible confusion in this case, let us note that we can set $w^* = 0$ after the limit $g_i \to 0$, $i = 1,2$, has been performed.

2. FPII

The results for fixed point FPII are nonuniversal with respect to parameter $a^*(w^*)$. Although this dependence is more instructive for results, it is more difficult for practical calculations. Therefore, in what follows we choose the independent parameter to be w^*. The relation between a^* and w^*, anomalous dimensions, and corresponding

$$a_\pm^*(w^*) = \frac{1}{2}\left(1 \pm \frac{\sqrt{X(w^*)}}{\sqrt{2}(w^*)}\right), \tag{C2}$$

where

$$X(w) = -3w^4 - 9w^3 - 3w^2 + 9w + 8. \tag{C3}$$

Note that two solutions (C2) correspond to two intersections of the curve (4) at fixed horizontal line $w^* = \text{const}$. If we consider $a^* \in \langle 0,1\rangle$, from Eq. (C2) we find that w^* ranges from 1 (at $a^* \in \{0,1\}$) to 1.0518(8) at $a^* = \frac{1}{2}$.

Eigenvalues of the Jacobi matrix are the following:

$$\lambda_5(w) = \frac{(6w^4 + 9w^3 + 9w + 16)}{6w(w+1)^3}, \tag{C4}$$

$$\lambda_6(w) = \frac{(9w^4 + 24w^3 + w^2 - 26w - 16)}{6w^3(w+1)}. \tag{C5}$$

There are two values for critical exponents due to the existence of two intersections of the curve $a^* = a^*(w^*)$ in Fig. 4:

$$\gamma_{\psi\pm}^* = \frac{(Y(w^*) \pm 4\sqrt{2}\sqrt{X(w^*)})}{12(w^*)^2((w^*)+1)}\varepsilon, \tag{C6}$$

$$\gamma_{\psi\pm}^* = \frac{(Y(w^*) \mp 4\sqrt{2}\sqrt{X(w^*)})}{12(w^*)^2((w^*)+1)}\varepsilon, \tag{C7}$$

$$\Theta = \frac{(3w^3 + 6w^2 - w - 8)}{12w^2(w+1)}\varepsilon, \tag{C8}$$

where

$$X(w) = -3w^4 - 9w^3 - 3w^2 + 9w + 8, \tag{C9}$$

$$Y(w) = -3w^4 - 6w^3 + w^2 + 8w. \tag{C10}$$

3. FPIV

Similarly to the fixed point FPII from previous section, for fixed point FPIV we have

$$a^*_{\pm} = \frac{1}{2}\left(1 + \frac{\sqrt{X(w^*)}}{2\sqrt{2}\alpha w^2(y-\epsilon)}\right), \tag{C11}$$

where

$$\begin{aligned} X = {} & \alpha w^2(y-\epsilon)(2\alpha w^2(y-\epsilon) - (w^2-1) \\ & \times \{y[4(\alpha+1) + (\alpha+2)w^2 + 3(\alpha+2)w] \\ & - \epsilon(2\alpha + 3w^2 + 9w + 6)\}). \end{aligned} \tag{C12}$$

Eigenvalues λ_5 and λ_6 from Table II are

$$\begin{aligned} \lambda_5(w,\Delta) = {} & \frac{1}{I}\{9(w+1)w^3\epsilon^2 + y^2[-8(\alpha+1) \\ & + 5(\alpha+2)w^4 + 10(\alpha+2)w^3 - (\alpha-2)w^2 \\ & - 2(5\alpha+8)w] + y\epsilon[4(\alpha+3) - 3(\alpha+7)w^4 \\ & - 3(\alpha+12)w^3 + (2\alpha-3)w^2 + 2(\alpha+12)w]\} \end{aligned} \tag{C13}$$

and

$$\begin{aligned} \lambda_6(w,\Delta) = {} & \frac{1}{I}\{y(y[8(\alpha+1) + 2(\alpha+2)w^4 3(\alpha+2)w^3 \\ & + 3(\alpha+2)w] - \epsilon[4(\alpha+3) \\ & + 6w^4 + 9w^3 + 9w])\}, \end{aligned} \tag{C14}$$

where the expression I is defined as follows:

$$I = 3w(w+1)^3[(\alpha+2)y - 3\epsilon]. \tag{C15}$$

4. FPIX

For the fixed point FPX, we have the following eigenvalues:

$$\lambda_5(y,\varepsilon) = \frac{A + \sqrt{6B}}{1200y}, \tag{C16}$$

$$\lambda_6(y,\varepsilon) = \frac{A - \sqrt{6B}}{1200y}, \tag{C17}$$

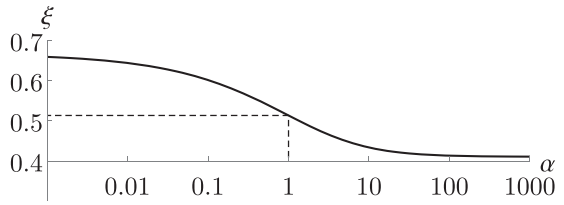

FIG. 10. The parameter ξ as a function of α. The results are consistent with the numerical solution shown in Fig. 5.

where we have used expressions

$$A = 48y^2 - 12y(C - 48\varepsilon) + 3\varepsilon(C + \varepsilon), \tag{C18}$$

$$\begin{aligned} B = {} & 145408y^4 + 3\varepsilon^3(C+\varepsilon) + 304y^2\varepsilon(11C + 377\varepsilon) \\ & - 12y\varepsilon^2(53C + 59\varepsilon) - 64y^3(53C + 3807\varepsilon), \end{aligned} \tag{C19}$$

$$C = \sqrt{176y^2 - 48y\varepsilon + \varepsilon^2}. \tag{C20}$$

5. Boundary between FPIV and FPV

In order to find the boundary between two nontrivial fixed points FPIV and FPV, we work in the ray scheme [76,77]. Since expansion parameters must be proportional, we relate them as

$$y = \frac{1}{\xi}\varepsilon. \tag{C21}$$

Now, we have to consider values of charges for both fixed points. According to our analytical and numerical solutions (see Table II and Fig. 5), charges g_3^* and a^* seem to converge at the boundary between FPIV and FPV. Hence, we may set $g_3^* = 0$ and $a^* = \frac{1}{2}$ during the calculation process. In this case, beta functions β_{g_3} and β_a vanish and coordinate w^* is found as a zero point of the function

$$\begin{aligned} \beta_w = {} & \frac{\varepsilon}{A}[w(w^3 + 3w^2 + w - 3)(\alpha - 3\xi + 2) \\ & + 2\alpha(\xi - 2) + 6\xi - 4], \end{aligned} \tag{C22}$$

where $A = 3\xi(w+1)^3(\alpha - 3\xi + 2)$. Note that $\xi < \frac{2}{3}$ since in the limit $\alpha \to 0$ the boundary between FPIV and FPV is simply $y = 3\varepsilon/2$. By calculating corresponding eigenvalues of the stability matrix, we find that $\lambda_7 = 0$, λ_6 is positive in the relevant region, and the line $\lambda_5(\xi,\alpha)/\varepsilon = 0$ is plotted in Fig. 10.

[1] B. Schmittmann and R. K. P. Zia, *Statistical Mechanics of Driven Diffusive Systems*, Vol. 17 of *Phase Transitions and Critical Phenomena* (Academic, New York, 1995).

[2] P. L. Krapivsky, S. Redner, and E. Ben-Naim, *A Kinetic View of Statistical Physics* (Cambridge University Press, Cambridge, 2010).

[3] U. C. Täuber, *Critical Dynamics: A Field Theory Approach to Equilibrium and Non-Equilibrium Scaling Behavior* (Cambridge University Press, Cambridge, 2014).

[4] D. J. Amit and V. Martín-Mayor, *Field Theory, the Renormalization Group and Critical Phenomena* (World Scientific, Singapore, 2005).

[5] J. Zinn-Justin, *Quantum Field Theory and Critical Phenomena* (Clarendon, Oxford, 1996).

[6] J. Zinn-Justin, *Phase Transitions and Renormalization Group* (Clarendon, Oxford, 2007).

[7] A. N. Vasil'ev, *The Field Theoretic Renormalization Group in Critical Behavior Theory and Stochastic Dynamics* (Chapman Hall/CRC, Boca Raton, FL, 2004).

[8] M. Henkel, H. Hinrichsen, and S. Lübeck, *Non-Equilibrium Phase Transitions: Volume 1-Absorbing Phase Transitions* (Springer, Berlin, 2008).

[9] J. Cardy and R. L. Sugar, J. Phys. A: Math. Gen. **13**, L423 (1980).

[10] S. P. Obukhov, Phys. A (Amsterdam) **101**, 145 (1980).

[11] H.-K. Janssen, Z. Phys. B **42**, 151 (1981).

[12] P. Grassberger, Z. Phys. B **47**, 365 (1982).

[13] G. Ódor, Rev. Mod. Phys. **76**, 663 (2004).

[14] H.-K. Janssen and U. C. Täuber, Ann. Phys. (NY) **315**, 147 (2005).

[15] P. Rupp, R. Richter, and I. Rehberg, Phys. Rev. E **67**, 036209 (2003).

[16] K. A. Takeuchi, M. Kuroda, H. Chaté, and M. Sano, Phys. Rev. Lett. **99**, 234503 (2007).

[17] M. Sano and K. Tamai, Nat. Phys. **12**, 249 (2016).

[18] G. Lemoult, L. Shi, S. V. Avila, K. Jalikop, M. Avila, and B. Hof, Nat. Phys. **12**, 254 (2016).

[19] H.-K. Janssen, K. Oerding, F. van Wijland, and H. Hilhorst, Eur. Phys. J. B **7**, 137 (1999).

[20] S. Rössner and H. Hinrichsen, Phys. Rev. E **74**, 041607 (2006).

[21] H. Hinrichsen, J. Stat. Mech. (2007) P07006.

[22] H. Hinrichsen, Adv. Phys. **49**, 815 (2000).

[23] H.-K. Janssen, Phys. Rev. E **55**, 6253 (1997).

[24] A. G. Moreira and R. Dickman, Phys. Rev. E **54**, R3090 (1996).

[25] R. Cafiero, A. Gabrielli, and M. A. Muñoz, Phys. Rev. E **57**, 5060 (1998).

[26] T. Vojta and M. Dickison, Phys. Rev. E **72**, 036126 (2005).

[27] T. Vojta and M. Y. Lee, Phys. Rev. Lett. **96**, 035701 (2006).

[28] L. T. Adzhemyan and N. V. Antonov, Phys. Rev. E **58**, 7381 (1998).

[29] N. V. Antonov, Phys. D (Amsterdam) **144**, 370 (2000).

[30] U. Frisch, *Turbulence: The Legacy of A.N. Kolmogorov* (Cambridge University Press, Cambridge, 1995).

[31] P. A. Davidson, *Turbulence: An Introduction for Scientists and Engineers*, 2nd ed. (Oxford University Press, Oxford, 2015).

[32] P. A. Davidson, Y. Kaneda, and K. R. Sreenivasan, *Ten Chapters in Turbulence* (Cambridge University Press, Cambridge, 2013).

[33] P. A. Davidson, Y. Kaneda, K. R. Moffatt, and K. Sreenivasan, *A Voyage Through Turbulence* (Cambridge University Press, Cambridge, 2011).

[34] N. V. Antonov, V. I. Iglovikov, and A. S. Kapustin, J. Phys. A: Math. Gen. **42**, 135001 (2009).

[35] N. V. Antonov, A. A. Ignatieva, and A. V. Malyshev, Phys. Part. Nuclei **41**, 998 (2010).

[36] N. V. Antonov, A. S. Kapustin, and A. V. Malyshev, Theor. Math. Phys. **169**, 1470 (2011).

[37] M. Dančo, M. Hnatič, T. Lučivjanský, and L. Mižišin, Theor. Math. Phys. **176**, 898 (2013).

[38] R. Kraichnan, Phys. Fluids **11**, 945 (1968).

[39] G. Falkovich, K. Gawędzki, and M. Vergassola, Rev. Mod. Phys. **73**, 913 (2001).

[40] L. T. Adzhemyan, N. V. Antonov, and A. N. Vasil'ev, *The Field Theoretic Renormalization Group in Fully Developed Turbulence* (Gordon & Breach, London, 1999).

[41] R. Benzi and D. R. Nelson, Phys. D (Amsterdam) **238**, 2003 (2009).

[42] S. Pigolotti, R. Benzi, M. H. Jensen, and D. R. Nelson, Phys. Rev. Lett. **108**, 128102 (2012).

[43] R. Volk, C. Mauger, M. Bourgoin, C. Cottin-Bizonne, C. Ybert, and F. Raynal, Phys. Rev. E **90**, 013027 (2014).

[44] M. De Pietro, M. A. T. van Hinsberg, L. Biferale, H. J. H. Clercx, P. Perlekar, and F. Toschi, Phys. Rev. E **91**, 053002 (2015).

[45] B. Delamotte, in *Renormalization Group and Effective Field Theory Approaches to Many-Body Systems. Lecture Notes in Physics*, edited by A. Schwenk and J. Polonyi (Springer, Berlin, 2012), Vol. 852.

[46] L. Canet, J. Phys. A: Math. Gen. **39**, 7901 (2006).

[47] L. Canet, H. Chaté, and B. Delamotte, J. Phys. A: Math. Theor. **44**, 495001 (2011).

[48] A. A. Fedorenko, P. L. Doussal, and K. J. Wiese, J. Stat. Mech. (2013) P04014.

[49] L. Canet, B. Delamotte, and N. Wschebor, Phys. Rev. E **93**, 063101 (2016).

[50] L. Canet, B. Delamotte, O. Deloubrière, and N. Wschebor, Phys. Rev. Lett. **92**, 195703 (2004).

[51] F. Benitez, C. Duclut, H. Chaté, B. Delamotte, I. Dornic, and M. A. Muñoz, Phys. Rev. Lett. **117**, 100601 (2016).

[52] K. J. Wiese, Phys. Rev. E **93**, 042117 (2016).

[53] C. De Dominicis, J. Phys. Colloq. **37**, C1-247 (1976).

[54] H. K. Janssen, Z. Phys. B **23**, 377 (1976).

[55] P. C. Martin, E. D. Siggia, and H. A. Rose, Phys. Rev. A **8**, 423 (1973).

[56] L. D. Landau and E. M. Lifshitz, *Fluid Mechanics: Landau and Lifshitz: Course of Theoretical Physics, Volume 6* (Elsevier, Amsterdam, 1987).

[57] A. S. Monin and A. M. Yaglom, *Statistical Fluid Mechanics Volume 1* (MIT Press, Cambridge, 1971).

[58] N. V. Antonov and A. S. Kapustin, J. Phys. A: Math. Gen. **43**, 405001 (2010).

[59] I. Staroselsky, V. Yakhot, S. Kida, and S. A. Orszag, Phys. Rev. Lett. **65**, 171 (1990).

[60] N. V. Antonov, M. Y. Nalimov, and A. A. Udalov, Theor. Math. Phys. **110**, 305 (1997).

[61] N. V. Antonov, N. M. Gulitskiy, M. M. Kostenko, and T. Lučivjanský, Phys. Rev. E **95**, 033120 (2017).

[62] M. Hnatič, J. Honkonen, and T. Lučivjanský, Acta Phys. Slov. **66**, 69 (2016).

[63] N. V. Antonov and M. M. Kostenko, Phys. Rev. E **90**, 063016 (2014).

[64] L. T. Adzhemyan, M. Y. Nalimov, and M. M. Stepanova, Theor. Math. Phys. **104**, 971 (1995).

[65] D. Y. Volchenckov and M. Y. Nalimov, Theor. Math. Phys. **106**, 307 (1996).

[66] N. V. Antonov, Phys. Rev. E **60**, 6691 (1999).

[67] N. V. Antonov, J. Phys. A: Math. Gen. **39**, 7825 (2006).

[68] N. V. Antonov, M. Hnatič, A. S. Kapustin, T. Lučivjanský, and L. Mižišin, Phys. Rev. E **93**, 012151 (2016).

[69] A. N. Vasil'ev, *Functional Methods in Quantum Field Theory and Statistical Physics* (Gordon and Breach, Amsterdam, 1998).

[70] K. Symanzik, Lett. Nuovo Cimento **8**, 771 (1973).
[71] R. Schloms and V. Dohm, Nucl. Phys. B **328**, 639 (1989).
[72] Wolfram Research, *Mathematica, Version 9.0* (Champaign, Illinois, 2012).
[73] K. Gawędzki and M. Vergassola, Phys. D (Amsterdam) **138**, 63 (2000).
[74] M. Hnatich, J. Honkonen, and M. Jurcisin, Phys. Rev. E **64**, 056411 (2001).
[75] J.-P. Bouchaud and A. Georges, Phys. Rep. **195**, 127 (1990).
[76] J. Honkonen and M. Y. Nalimov, Z. Phys. B **99**, 297 (1995).
[77] L. T. Adzhemyan, J. Honkonen, M. V. Kompaniets, and A. N. Vasil'ev, Phys. Rev. E **71**, 036305 (2005).